Members of the Rusc protein family interact with Sufu and inhibit vertebrate Hedgehog signaling

Zhigang Jin[a], Tyler Schwend[a, b], Jia Fu[a], Zehua Bao[c], Jing Liang[c, d], Huimin Zhao[c], Wenyan Mei[a], Jing Yang[a, 1]

[a]Department of Comparative Biosciences, University of Illinois at Urbana-Champaign, 2001 S Lincoln Avenue, Urbana, IL 61802 USA

[b]Current address: CNS C109A, Illinois Wesleyan University, Bloomington, IL 61702 USA

[c]Department of Chemical and Biomolecular Engineering, University of Illinois at Urbana-Champaign, 600 South Mathews Avenue, Urbana, IL 61801 USA

[d]Current address: Metabolic Engineering Research Laboratory, Science and Engineering Institutes, 31 Biopolis Way, the Nanos, Singapore 138669

[1]Corresponding author: Jing Yang (yangj@illinois.edu)

Key words: Hedgehog Signaling, Sufu, Rusc, Gli, Development, *Xenopus*

Summary Statement

Rusc proteins are novel components of the vertebrate Hedgehog pathway. They bind Sufu and inhibit Hh signaling by preventing signaling-induced dissociation of Sufu and Gli.

Abstract

Hedgehog (Hh) signaling is fundamentally important for development and adult tissue homeostasis. It is well established that in vertebrates, Sufu directly binds and inhibits Gli proteins, the downstream mediators of Hh signaling. However, it is unclear how the inhibitory function of Sufu toward Gli is regulated. Here we report that the Rusc family of proteins, whose biological functions are poorly understood, form a heterotrimeric complex with Sufu and Gli. Upon Hh signaling, Rusc is displaced from this complex, followed by dissociation of Gli from Sufu. In mammalian fibroblast cells, knockdown of Rusc2 potentiates Hh signaling by accelerating signaling-induced dissociation of the Sufu-Gli protein complexes. In *Xenopus* embryos, knockdown of Rusc1 or overexpression of a dominant negative Rusc enhances Hh signaling during *Xenopus* eye development, leading to severe eye development defects. Our study thus uncovers a novel regulatory mechanism controlling the response of cells to Hh signaling in vertebrates.

Introduction

The Hedgehog (Hh) signaling pathway is evolutionarily conserved and involved in a wide variety of processes during embryogenesis and adult tissue homeostasis (Jiang and Hui, 2008; Hui and Angers, 2011; Briscoe and Therond, 2013; Petrova and Joyner, 2014). One of the most important roles that Hh signaling plays during vertebrate early development is patterning of the neural tube. It is well established that ventrally derived Sonic hedgehog (Shh) gradient counteracts dorsally derived Wnts and BMPs gradients, determining fates of cells along the dorsal ventral axis of the neural tube (Lupo et al., 2006; Briscoe, 2009; Briscoe and Small, 2015). In the anterior neural ectoderm, Hh signaling is essential for the formation of eye primordia. During eye development, the eye primordium is initially specified as a single morphogenetic field in the anterior neural plate. Shh, which is secreted by the prechordal plate, suppresses the expression of eye specific genes in the midline and divides the eye field into two lateral eye primordia. Inhibition of Shh signaling impairs the eye separation process and induces cyclopia. In contrast, increased Shh signaling reduces the size of the eye (Amato et al., 2004). Proper response of cells to Shh is critically important for these developmental processes.

At the molecular level, zinc finger transcription factor Cubitus interruptus (Ci) and its vertebrate homologues Gli proteins act at the downstream end of the pathway to mediate Hh signaling in Drosophila and vertebrates, respectively. In un-stimulated cells, multiple inhibitory mechanisms act in coordination to keep Ci/Gli in check. The Hh family of proteins operates the pathway by relieving these inhibitory mechanisms, which ultimately converts Ci and Gli into transcriptional activators and induces expression of Hh target genes. Interfering with these Hh inhibitory mechanisms often causes severe consequences, ranging from defective embryonic development to tumorigenesis (Huangfu and Anderson, 2006; Jia and Jiang, 2006; Jiang and Hui, 2008; Hui and Angers, 2011; Briscoe and Therond, 2013; Petrova and Joyner, 2014).

In vertebrates, one of the major Hh inhibitory mechanisms is mediated by suppressor of fused (Sufu). Sufu deficiency leads to constitutive pathway activation, resulting in severe patterning defects during development (Cooper et al., 2005; Svard et al., 2006; Min et al., 2011). Mouse embryos homozygous for the *Sufu* null allele die around E9.5 with severely ventralized neural

tubes that remain open in the anterior region (Svard et al., 2006). Knockdown of Sufu in *Xenopus* embryos also increases the expression of Hh target genes. As expected, Sufu depleted *Xenopus* embryos develop severely reduced eyes (Min et al., 2011). In humans, inherited and sporadic mutations in Sufu have been identified in a wide variety of cancers, including medulloblastoma (Taylor et al., 2002; Brugieres et al., 2010), meningioma (Aavikko et al., 2012), and basal cell carcinoma (Pastorino et al., 2009; Kijima et al., 2012; Schulman et al., 2015). Interestingly, different from Sufu in other vertebrate species, zebrafish Sufu is a weak Hh inhibitor. Knockdown of Sufu causes only a marginal increase in Hh signaling during zebrafish embryonic development (Wolff et al., 2003).

At the molecular level, Sufu directly binds Gli proteins when the Hh pathway is quiescent (Ding et al., 1999; Kogerman et al., 1999; Pearse et al., 1999; Stone et al., 1999; Zhang et al., 2013; Han et al., 2015). Sufu can inhibit Gli-dependent transcription through sequestering Gli proteins in the cytoplasm (Ding et al., 1999; Kogerman et al., 1999; Murone et al., 2000; Han et al., 2015). In the nucleus, Sufu recruits the NuRD repressor complex member p66ß to the promoters of Hh target genes and suppresses Gli-dependent transcription (Lin et al., 2014). Binding of Hh ligands to their receptors triggers dissociation of the Sufu-Gli protein complexes. This relieves the inhibitory effects of Sufu on Gli proteins and allows conversion of Gli proteins into transcriptional activators, which induce the expression of Hh target genes (Humke et al., 2010; Tukachinsky et al., 2010; Zeng et al., 2010; Lin et al., 2014). Interestingly, Sufu regulates the stability of Gli proteins as well. In the absence of Sufu, although Gli proteins become hyperactive, the total level of Gli proteins is markedly reduced (Chen et al., 2009; Jia et al., 2009; Wang et al., 2010; Liu et al., 2012). It is believed that Sufu prevents Spop-dependent proteasome degradation of Gli proteins (Wang et al., 2010). While the important roles that Sufu plays in vertebrate Hh signaling are well established, it is less clear how the inhibitory function of Sufu toward Gli proteins is regulated.

The RUN and SH3 domain-containing (Rusc) family is a small vertebrate protein family consisting of two family members. Rusc1 and Rusc2 both contain a RUN domain and a C-terminal SH3 domain. The shortest isoform of Rusc1, namely Nesca, is involved in the neurotrophin signaling pathway (MacDonald et al., 2012; Sun et al., 2012). The function of Rusc2 is completely unknown. In this study, we report that Rusc1 and Rusc2 interact with Sufu and restrict the response of cells to Hh signaling.

Results

Members of the Rusc family interact with Sufu and inhibit Hh signaling

Rusc2 was identified from a yeast-2 hybrid screen using the full-length Sufu as bait. To verify the interaction between Sufu and Rusc2, we performed a co-immunoprecipitation in HEK293T cells. We were able to co-immunoprecipitate FLAG-tagged hRusc2 with myc-hSufu (Fig. 1A, upper panel). In the reverse CoIP, myc-hSufu co-purified with hRusc2-FLAG (Fig. 1A, lower panel). Furthermore, we detected interaction between endogenous Rusc2 and Sufu in mouse brain (Fig. 1B). Members of the Rusc protein family are highly similar to each other (Fig. 1C). Our results reveal that like hRusc2, mRusc1 interacted with hSufu (Fig. 1D). In addition, *Xenopus* Rusc1 (Fig. 1E) and Rusc2 (Fig. 1F) both interacted with hSufu.

To study the functions of Rusc proteins in Hh signaling, we took advantage of a Hh-responsive luciferase reporter (8xGli-BS luciferase (Sasaki et al., 1997)). As expected, Gli1 and Gli2 activated 8xGli-BS luciferase in NIH3T3 cells. Overexpression of mRusc1 or hRusc2 markedly reduced the activity of Gli1 and Gli2 in this assay (Fig. 2A). Interestingly, only *rusc2* is abundantly expressed in NIH3T3 and mouse embryonic fibroblasts (MEFs) (S-Fig. 1). We thus knocked down Rusc2 using two shRNAs, which target different regions of *rusc2* mRNA (Fig. 2B). As shown in Fig. 2C, knockdown of Rusc2 in MEFs markedly enhanced Shh-induced expression of *gli1* and *ptc1*, two direct targets of Hh signaling. Consistently, knockdown of Rusc2 increased Gli1- and Gli2-induced 8xGli-BS luciferase activities (Fig. 2D). Similar results were obtained when the experiment was performed in NIH3T3 cells (data not shown). In addition to shRNA knockdown experiments, we took advantage of the transcription activator-like effector nuclease (TALEN) technology and generated a rusc2 heterozygous mutant MEF cell line (S-Fig. 2A and B). Compared to control MEFs, rusc2 heterozygous mutant MEFs exhibited a more robust response to overexpressed Gli1 (S-Fig. 2C and D) or Shh-N conditioned medium (S-Fig. 2E and F). These results demonstrate that Rusc2 inhibits Hh signaling.

Next we carried out a systematic epistasis analysis. As shown in Fig. 2E, overexpression of hRusc2 inhibited Gli1-induced 8xGli-BS luciferase in IFT88 knockout MEFs, which are deficient in primary cilia (Murcia et al., 2000). This demonstrates that Rusc2 functions independent of cilium in the Hh pathway. To define the epistatic relationship between Rusc2

and Sufu, we assayed the activity of Sufu in wild type and Rusc2 knockdown MEFs. Sufu reduced Gli1-induced 8xGli-BS luciferase activity in the wild type and Rusc2 knockdown MEFs (Fig. 2F), indicating that Sufu can inhibit Hh signaling independent of Rusc2. In contrast, knockdown of Rusc2, which enhanced Shh conditioned medium-induced expression of *gli1* and *ptc1* in the wild type MEFs, failed to do so in Sufu knockout MEFs (Fig. 2G). Consistently, overexpression of hRusc2 reduced Gli1-induced 8xGli-BS luciferase activity in wild type MEFs, but not in Sufu knockout MEFs (Fig. 2H). These results demonstrate that Rusc2 regulates the Hh pathway at the level of Gli. In addition, Sufu is required for the function of Rusc2 in Hh signaling.

Rusc2 inhibits signaling-induced dissociation of Sufu and Gli

Sufu directly binds and inhibits Gli proteins. Since Rusc proteins interact with Sufu and inhibit Gli, we determined if Rusc2 could form complexes with Gli proteins. Indeed, FLAG-hRusc2 co-immunoprecipitated with all three Gli proteins in HEK293T cells (Fig. 3A). We found that Sufu is required for the interaction between Rusc2 and Gli proteins. In Sufu knockout MEFs, we could not detect binding between Rusc2 and Gli3 (Fig. 3B). Interestingly, we could not detect binding between Rusc2 and Sufu^{R362C}, an oncogenic form of Sufu deficient in Gli binding (Fig. 3C). Moreover, overexpression of mSpop, which promotes proteasome-dependent degradation of Gli proteins (Zhang et al., 2006; Zhang et al., 2009), reduced the binding between hRusc2 and hSufu in a dose dependent manner (Fig. 3D). These results suggest that Rusc2 preferentially binds Sufu that is associated with Gli proteins.

In vertebrates, Hh signaling induces translocation of the Sufu-Gli complex to the primary cilium and subsequent dissociation of the Gli-Sufu complexes. This converts Gli proteins into Gli activators that activate Hh-dependent transcription (Humke et al., 2010; Tukachinsky et al., 2010; Zeng et al., 2010; Lin et al., 2014). Since Rusc2, Sufu, and Gli form a heterotrimeric complex, we investigated the effect of Hh signaling on this protein complex. We treated MEFs with a low dose of Shh-N conditioned medium, which triggered the Hh pathway with slow activation kinetics. We then performed CoIP to measure the amount of endogenous Gli3 and Rusc2 that were associated with endogenous Sufu. In un-stimulated MEFs, Rusc2 and Gli3 co-immunoprecipitated with Sufu. In MEFs treated with Shh conditioned medium for 3 hours, we could not detect binding between Sufu and Rusc2. By contrast, Sufu and Gli3 remained associated with each other at this time point. At 6 hours post Shh conditioned medium treatment, the Sufu-Gli3 complex was dissociated (Fig. 4A).

This indicates that the Rusc2-Sufu-Gli complex is dissociated sequentially upon Hh signaling, with dissociation of Rusc2 occurring prior to the collapse of the Gli-Sufu protein complex.

We extended our analysis by assessing the subcellular localization of Rusc2. In un-stimulated cells, Rusc2 protein was mainly detected in the cytoplasm. A small amount of Rusc2 protein overlapped with γ-Tubulin, a marker for cilia basal bodies (Fig. 4B, B', and B"). This localization pattern remained unchanged in cells treated with Shh conditioned medium (Fig. 4C, C', and C"). This is in stark contrast to Gli3, which is translocated to the tip of the cilium upon Shh-N conditioned medium treatment (Fig. 4F and G). Dissociation of Sufu and Gli occurs after their ciliary translocation (Tukachinsky et al., 2010; Zeng et al., 2010). Lack of ciliary translocation of Rusc2 upon Hh signaling thus further supports the idea that Hh signaling induces sequential dissociation of the Rusc2-Sufu-Gli protein complex.

In light of the above findings, we set out to determine if Rusc2 prevents signaling-induced dissociation of the Sufu-Gli protein complexes. After titrating the dose of Shh-N conditioned medium, we chose to treat MEFs with a low dose of Shh-N conditioned medium. This treatment was insufficient for inducing the expression of *ptc1*, and caused only a 3-fold increase in the expression of *gli1* at 16 hours. When Rusc2 knockdown MEFs were treated with the same dose of Shh-N conditioned medium, a significant increase in the expression of *gli1* and *ptc1* was detected at 8 hours after addition of Shh-N conditioned medium. At 16 hours post treatment, we detected a robust increase in the expression of both *gli1* and *ptc1* (Fig. 4H). Under the same treatment condition, we performed Sufu CoIP to assess the effects of Rusc2 knockdown on the Sufu-Gli protein complexes. In un-stimulated MEFs, knockdown of Rusc2 did not alter the interaction between Gli3 and Sufu, although a marginal reduction in the amount of Gli3 coimmunoprecipitated with Sufu was occasionally observed. At 8 hours post Shh-N conditioned medium treatment, Gli3 and Sufu remained associated with each other in control MEFs. In Rusc2 knockdown MEFs, however, we could no longer detect binding between Gli3 and Sufu (Fig. 4I). This demonstrates that knockdown of Rusc2 accelerates dissociation of the Sufu-Gli protein complexes upon Hh signaling. Knockdown of Rusc2 did not alter the subcellular localization of Gli in un-stimulated MEFs (S-Fig. 3). Taken together, we conclude that Rusc2 inhibits Hh signaling by preventing signaling induced dissociation of the Sufu-Gli protein complexes.

Overexpression of Rusc2 induces cytoplasmic Gli protein aggregates

Next we compared the activities of Sufu and Rusc2 in regulating the expression and subcellular localization of Gli proteins. We found that overexpression of Sufu, but not Rusc2, increased the level of Gli proteins (Fig. 5A). Both Sufu and Rusc2 reduced the activities of Gli1 and Gli2 in an 8xGli-BS luciferase reporter assay. However, the activity of Rusc2 is less potent in this assay (Fig. 5B). When expressed alone in NIH3T3 cells, Gli3 was enriched in the nucleus. When Gli3 and Sufu were co-expressed, the level of Gli3 was increased dramatically and the majority of Gli3 proteins were detected in the cytoplasm. Overexpression of Rusc2 decreased the amount of nuclear Gli3 too, albeit to a lesser extent. Strikingly, overexpressed Rusc2 induced large Gli3 protein aggregates in the cytoplasm (Fig. 5C). Similar results were obtained when Gli1 and Gli2 were co-expressed with Rusc2 (S-Fig. 4). Strikingly, these cytoplasmic Gli protein aggregates are resistant to extraction with Triton X-100. We found that Sufu can induce Triton resistant cytoplasmic Gli3 protein aggregates too, albeit its activity is weaker (Fig. 5C and S-Fig. 4B). We further determined if Sufu was required for Rusc2 to induce cytoplasmic Gli protein aggregates. In wild type MEFs, overexpression of Rusc2 resulted in cytoplasmic retention of Gli3 and induced cytosolic Gli3 protein aggregates. In Sufu knockout MEFs, however, overexpressed Rusc2 did not cause relocalization of Gli3 or induce Gli3 protein aggregates. Gli3 protein remained in the nucleus (Fig. 5D and S-Fig. 4C). This indicates that Rusc2 regulates subcellular distribution of Gli proteins in a Sufu-dependent manner. This finding further supports the idea that Rusc2 modulate the Hh pathway by regulating the interaction between Sufu and Gli.

Rusc1 inhibits Hh signaling during *Xenopus* embryonic development

To understand the in vivo functions of Rusc proteins, we examined the expression of *rusc1* and *rusc2* in *Xenopus* embryos. *Rusc1* is expressed maternally and is present abundantly and ubiquitously in the embryo. Maternal *rusc1* mRNA declines gradually during the gastrula and neurula stages (Fig. 6A and B). By the late neurula stage, strong expression of *rusc1* was detected in the developing neural tube and eye domains (Fig. 6B). At this stage, the eye domains, which strongly express *rusc1*, do not express *gli1*, a direct target of Hh signaling (Lee et al., 1997) (Fig. 6B). This raises the possibility that Rusc1 may inhibit Hh signaling in the developing eye. As development proceeded, maternal *rusc1* further declines. At the late tailbud stage, strong expression of *rusc1* is observed in the dorsal neural tube, eyes, and branchial arches (Fig. 6B). Different from *rusc1*, *rusc2* expression commences zygotically.

We could not detected *rusc2* by in situ hybridization at stage 14 (data not shown). Starting from stage 18, the expression of *rusc2* can be detected in Rohon-Beard neurons, which are located along the dorsal neural tube in the trunk region. In the anterior region, *rusc2* is specifically expressed in the trigeminal ganglion. At stage 33, in addition to Rohon-Beard neurons and trigeminal ganglion (black arrow), *rusc2* is expressed in the middle lateral line placode (red arrow) and anterodorsal lateral line placode (yellow arrow) (Fig. 6B).

To study functions of Rusc proteins during development, we first took a dominant negative approach. We generated multiple hRusc2 deletion constructs (Fig. 7A) and characterized the interaction between Rusc2 and Sufu in greater detail. We found that the full-length hRusc2, Rusc$^{608\text{-}903}$, and Rusc$^{1233\text{-}C}$ interacted with hSufu in HEK293T cells (Fig. 7A and B) and in the yeast-2 hybrid system (data not shown). When Rusc$^{1233\text{-}C}$ was overexpressed, it interfered with complex formation between the full-length hRusc2 and hSufu in a dose-dependent manner (Fig. 7C). We overexpressed Rusc$^{1233\text{-}C}$ in NIH3T3 cells and performed an 8xGli-BS luciferase reporter assay. In stark contrast to the full-length hRusc2, which inhibited Gli1 and Gli2, Rusc$^{1233\text{-}C}$ markedly enhanced the activities of Gli1 and Gli2 in the 8xGli-BS luciferase assay (Fig. 7D). This indicates that Rusc$^{1233\text{-}C}$ acts as a dominant negative Rusc.

It is well established that Shh separates the eye field into two distinct eye primordia by suppressing the expression of eye specific genes in the midline. Elevated Hh signaling often reduces the expression of eye markers and decreases the size of the eye (Amato et al., 2004; Koide et al., 2006; Rorick et al., 2007; Min et al., 2011). We injected Rusc$^{1233\text{-}C}$ (1 ng) at the 8-cell stage into dorsal animal blastomeres, which give rise to the neural tube and retina (Moody, 1987; Moody, 2012). To assess changes in Hh signaling, we monitored the expression of *gli1*, a direct target of Hh signaling (Lee et al., 1997). Indeed, overexpression of Rusc$^{1233\text{-}C}$ increased the expression of *gli1* in cells located close to the midline in the neural ectoderm (61%, n=123) (Fig. 7E). This was accompanied by a severe reduction in the expression of eye markers, including *pax6* (72%, n=25), *rax* (67%, n=31), and *six3* (68%, n=25) (Fig. 7E). At the late tailbud stage, the majority of Rusc$^{1233\text{-}C}$ overexpressed embryos (86%, n=64) exhibited reduced eyes (Fig. 7F). Thus, overexpression of a dominant negative Rusc enhances Hh signaling and impairs *Xenopus* eye development.

We then designed morpholinos, which blocked translation of *Xenopus rusc1* and *rusc2* in embryos (S-Fig. 5A). Injection of these morpholinos (20 ng) into both dorsal blastomeres at

the 4-cell stage had distinct effects on early development. We did not detect any morphological abnormalities in *rusc2* morpholinos (R2-MO) injected embryos. In contrast, injection of *rusc1* morpholino (R1-MO) induced severe defects during development. Compared to un-injected controls or embryos injected with 5-base mismatch morpholino (R1-5mis), R1-MO injected embryos showed shorter anterior-posterior axis and severely reduced eyes (Fig. 8A). Histological analysis reveals that knockdown of Rusc1 did not abolish the eye completely. Retina tissues are present even in embryos with severely disrupted eyes (S-Fig. 5B). Both the eye and A/P axis defects induced by R1-MO were rescued by injection of myc-Rusc1 (1 ng) (Fig. 8B). To further test the specificity of Rusc1 knockdown, we designed another morpholino (R1-sb), which blocks the splicing of *rusc1*. Similar to phenotypes observed in R1-MO injected embryos, R1-sb injected embryos showed reduced eyes and shortened A/P axis (S-Fig. 6A-C). We thus conclude that Rusc1 is essential for *Xenopus* development.

To determine if Rusc1 inhibits Hh signaling during development, we took advantage of the animal cap assay, an in vitro assay for studying Hh signaling in *Xenopus* embryonic tissues (Rorick et al., 2007; Min et al., 2011; Schwend et al., 2013). In Chordin (Chd) neuralized animal caps, injection of R1-MO caused a two-fold increase in the expression of *gli1*, *ptc2*, and *Hhip* at stage 22 and a modest increase in the expression of *ptc1* (Fig. 8C). This demonstrates that knockdown of Rusc1 increases the expression of Hh target genes. In whole embryo, injection of R1-MO had no effect on eye specific gene expression at stage 14 (data not shown). From the late neurula stage, we began to observe reduction in the expression of eye markers. These include *pax6* (45%, n=31), *rax* (36%, n=33), and *six3* (47%, n=30). Knockdown of Rusc1 increased the expression of *gli1* in cells located close to the midline in the neural ectoderm (54%, n=54), without altering the expression of *shh* (Fig. 8D). The eye defect induced by Rusc1 knockdown became more pronounced by the late tailbud stage, with the expression of *pax6* (81%, n=27), *rax* (81%, n=31), and *six3* (77%, n=26) being reduced in the majority of R1-MO injected embryos. Interestingly, the expression of *pax6* in the dorsal neural tube was affected to a lesser extent, even in embryos with severely reduced eyes. We again assessed the Hh signaling activity by monitoring the expression of *gli1*. While the head was generally small on the R1-MO injected side, 58% of the injected embryos (n=38) exhibited nearly uniform expression of *gli1* on the injected side. This is distinct from the uninjected side, where a "*gli1*-free" eye domain is prominent (Fig. 8E, pointed by arrowhead). Knockdown of Rusc1 by injection of R1-sb induced similar phenotypes (S-Fig.

6E). Since overexpression of the dominant negative Rusc and knockdown of Rusc1 both increase *gli1* expression and impair eye formation, we conclude that Rusc1, which is strongly expressed in the developing eye, inhibits Hh signaling during eye development.

To determine if the eye defects induced by Rusc1 knockdown could be attributed to elevated Hh signaling, we knocked down Gli1 in Rusc1 depleted embryos. Unilateral knockdown of Rusc1 induced eye defects in 95% of embryos (42% had severe defects and another 53% had milder eye defects (n=45)). Interestingly, 73% of injected embryos had their bodies bent toward the injected side, likely due to shortened A/P axis on the injected side. Co-injection of Gli1 morpholino (Nguyen et al., 2005; Schwend et al., 2013) clearly rescued the Rusc1 knockdown phenotypes, with the majority of embryos (96%, n=45) developing a straight body axis and only 16% of embryos showed mildly affected eyes (Fig. 8F). This demonstrates that the eye developmental defects observed in Rusc1 knockdown embryos are indeed a consequence of enhanced Hh signaling in these embryos.

Discussion

Although the Hh pathway is evolutionarily conserved, many differences exist between vertebrate and Drosophila Hh signaling (Huangfu and Anderson, 2006; Wilson and Chuang, 2010). One major difference is Sufu, which is dispensable for Drosophila Hh signaling (Preat, 1992), but functions as a major pathway inhibitor in vertebrates (Cooper et al., 2005; Svard et al., 2006; Min et al., 2011). Sufu physically interacts with Gli proteins and regulates their stability, localization, and activities (Ding et al., 1999; Kogerman et al., 1999; Murone et al., 2000; Lin et al., 2014; Han et al., 2015). Loss of Sufu elevates vertebrate Hh signaling and induces severe patterning defects during development (Wolff et al., 2003; Cooper et al., 2005; Svard et al., 2006; Min et al., 2011). In humans, oncogenic mutations in Sufu have been identified from medulloblastoma, basal cell carcinoma, and other cancers (Taylor et al., 2002; Pastorino et al., 2009; Brugieres et al., 2010; Aavikko et al., 2012; Kijima et al., 2012; Schulman et al., 2015). Despite the fundamental roles played by Sufu in development and cancer, it is largely unclear how Sufu protein itself is regulated.

Here we report that members of the Rusc protein family, which exists in vertebrates, but not in Drosophila, are novel Sufu-binding partners. Both Rusc1 and Rusc2 bind Sufu and inhibit Hh signaling. In the case of Rusc2, a domain located upstream of the RUN domain and the C-terminal SH3 domain are responsible for binding Sufu. During *Xenopus* development, Rusc1 is expressed predominantly. Rusc1 is expressed maternally. Zygotic Rusc1 is strongly expressed in the developing eyes and the neural tube. Overexpression of a dominant negative Rusc or knockdown of Rusc1 leads to increased Hh signaling, which impairs eye development. Knockdown of Rusc2, whose expression is restricted to only a few lineages, does not cause any detectable morphological defects. Different from *Xenopus* embryos, NIH3T3 and MEFs express Rusc2 predominantly. Knockdown of Rusc2 in these cells potentiates Hh signaling. These findings demonstrate that Rusc1 and Rusc2 are novel components of the vertebrate Hh pathway.

Our results reveal that Rusc2 exerts its inhibitory effect on Hh signaling through binding Sufu. As the major Gli inhibitor, Sufu forms complexes with Gli proteins and sequesters Gli proteins in the cytoplasm (Ding et al., 1999; Kogerman et al., 1999; Pearse et al., 1999; Stone et al., 1999; Zhang et al., 2013; Han et al., 2015). In the nucleus, Sufu recruits p66ß to the promoters of Hh target genes and represses Gli-dependent transcription (Lin et al., 2014). Hh signaling dissociates the Sufu-Gli protein complexes, converting Gli proteins into transcriptional activators, which ultimately activate the expression Hh target genes (Humke et al., 2010; Tukachinsky et al., 2010; Zeng et al., 2010; Lin et al., 2014). Our results reveal that Rusc2, Sufu, and Gli form a heterotrimeric protein complex. Upon Hh signaling, this complex is dissociated sequentially, with Rusc2 falling off from the complex first, followed by dissociation of Gli from Sufu. While knockdown of Rusc2 is insufficient for pathway activation, it potentiates Hh signaling by accelerating signaling-induced dissociation of the Sufu-Gli complexes. It is important to note that Sufu is required for the function of Rusc2 in the Hh pathway. In the absence of Sufu, knockdown or overexpression of Rusc2 has no effects on the output of Hh signaling. These observations strongly argue that Rusc2 function in the Hh pathway by stabilizing the Sufu-Gli protein complexes. In support of this hypothesis, we found that overexpression of Rusc2 decreases the amount of Gli proteins in the nucleus, and induces cytosolic Gli protein aggregates, which are resistant to Triton extraction. This activity of Rusc2 is again Sufu-dependent. It appears that Rusc2 inhibits Hh signaling by binding Sufu and stabilizing the Sufu-Gli protein complexes.

Notably, the functions of Rusc differ in several aspects from that of Sufu. Sufu deficiency results in robust pathway activation and destabilization of Gli proteins (Svard et al., 2006; Chen et al., 2009; Jia et al., 2009; Wang et al., 2010). In contrast, knockdown or overexpression of Rusc2 has no effect on the stability of Gli proteins. Knockdown of Rusc2 alone does not activate the Hh pathway. Elevated Hh signaling occurs only when cells are stimulated. In overexpression studies, Sufu sequesters Gli proteins in the cytoplasm very potently and inhibits Gli-dependent transcription. The activity of Rusc2 is weaker in these assays. Interestingly, Rusc2 is capable of inducing large cytoplasmic Gli protein aggregates. Although Sufu is required for this activity of Rusc2, Sufu itself has a weak activity in inducing cytosolic Gli protein aggregates. These findings are consistent with our hypothesis that Rusc2 stabilizes the Sufu-Gli protein complexes.

In *Xenopus*, knockdown of Rusc1 enhances Hh signaling and impairs eye development, which is reminiscent of the Sufu loss-of-function phenotypes. Nevertheless, the defects induced by Rusc1 knockdown are less severe than phenotypes observed in Sufu knockdown embryos. Sufu deficient *Xenopus* embryos show a robust Hh activation. Increased expression of *ptc1* was detected as early as the early neurula stage (stage 15) (Min et al., 2011). In Rusc1 knockdown embryos, however, we began to detect an increase in the expression of *gli1*, which is very sensitive to Hh signaling, from the late neurula stage. The expression of *ptc1* was increased only moderately. This suggests that knockdown of Rusc1 only causes a weak Hh activation in embryos. These functional differences between Sufu and Rusc are again in agreement with the view that Rusc proteins regulate the Hh pathway by enhancing the inhibitory functions of Sufu.

Interestingly, Rusc proteins interact with kinesins (MacDonald et al., 2012) and Rab family members (Bayer et al., 2005; Fukuda et al., 2011). In vertebrates, Kif7, a member of the kinesin protein family, interacts with Gli proteins and plays an important role in Hh signaling (Tay et al., 2005; Cheung et al., 2009; Endoh-Yamagami et al., 2009; Liem et al., 2009; Law et al., 2012; Li et al., 2012; He et al., 2014). Zebrafish Kif7 potentiates the activity of Gli2 by promoting its dissociation from Sufu (Maurya et al., 2013). It is also known that Rab23, which regulates endocytic and ciliary trafficking (Evans et al., 2003; Boehlke et al., 2010), is highly expressed in the dorsal neural tube and regulates Hh signaling during neural tube patterning (Eggenschwiler et al., 2001; Li et al., 2007). Similar to Rusc proteins, Rab23

functions downstream of Smo and PTCH and inhibits Gli1 in a Sufu-dependent manner (Evans et al., 2003; Eggenschwiler et al., 2006; Chi et al., 2012). In the future, it will be of great interest to determine if Rusc proteins physically and functionally interact with Kif7 or Rab23 in Hh signaling.

Materials and Methods

Yeast two-hybrid screen

An adult mouse brain cDNA library (Clontech) was screened using full-length hSufu (pGBKT7-hSufu) as bait, according to standard protocols (Yeast Protocols Handbook, Clontech).

Plasmids

Gli1, Gli2, Gli3, hSufu (Schwend et al., 2013), and hRusc2 (Bayer et al., 2005) expression constructs were reported. Mouse Rusc1 was constructed by PCR from IMAGE:6816267. *Xenopus* Rusc1 and Rusc2 were identified by blasting *Xenopus laevis* genome using mammalian Rusc proteins. xRusc1 (KX265097) and xRusc2 (KX265098) were PCR cloned from *Xenopus* cDNA. All deletion constructs were generated by PCR and standard cloning methods. Sufu^{R362C} mutant was generated by site-directed mutagenesis. Cloning details will be provided upon request.

Cell lines, shRNAs, transfection, and conditioned medium treatments

NIH3T3, HEK293T, and MEFs cells were cultured and transfected as described (Jia et al., 2009; Jin et al., 2010). Sufu-/- and IFT88-/- MEFs were provided by Dr. A. Liu. The Rusc2 heterozygous mutant MEF cell line was generated by transfection of a TALEN pair targeting the second exon of mouse Rusc2 gene as previously described (Mussolino et al., 2011). The targeting sequences of the Rusc2 loci are 5'-TTCTACCTGGACCTGCAGC-3' and 5'-TGTCTTGCGAGTCCCACCA-3', with a spacer (5'-cctccccggctgagtcgagaa-3'). TALEN transfected MEFs were selected with puromycin. A Rusc2 heterozygous mutant MEF cell line derived from TALEN transfected single cells were established.

Lentiviral shRNA constructs (TRCN0000252575 (targeting 5'-aggccatatccatcgacatac-3') and TRCN0000252578 (targeting 5'-gtccactaggccgactgataa-3')) were purchased from Sigma-

Aldrich. Lentiviral shRNA constructs were cotransfected into HEK293T cells with the virus packaging plasmids pCMV-ΔR and VSV-G for virus preparation. Lentiviral particles containing supernatant was collected at 48 h post-transfection. Virus infection was carried out by adding virus-containing supernatant into cell culture. After infection, cells were selected with 2 μg/ml puromycin.

Shh-N conditioned medium was prepared from Shh-N transfected HEK293T cells. One day after transfection, medium was replaced with DMEM containing 2% FBS and was collected and filtered through a 0.22-μm membrane after additional 2 days. Medium collected from non-transfected HEK293T cells served as control. To test the activity of each preparation, we treated NIH3T3 cells with Shh-N conditioned medium and performed RT-PCR for *ptc1* and *gli1*. For conditioned medium treatment, cells were starved in DMEM containing 0.5% FBS for 24 hours, treated with control or Shh-N conditioned medium, and harvested at desired time points.

Co-immunoprecipitation, Western blots, luciferase assay, and immunofluorescence

Antibodies used in this study were: anti-Rusc2 (#AP12095a, Abgent), anti-myc (#5546, Sigma-Aldrich), anti-FLAG (#F1804, Sigma-Aldrich), anti-HA (#H9658, Sigma,), anti-Sufu (#sc-28847 and #sc-10934, Santa Cruz), anti-Gli3 (#AF3690, R&D System) and anti-acetylated tubulin (#T7451, Sigma-Aldrich), anti-γ-tubulin (#T6557, Sigma-Aldrich), and anti-β-tubulin (#T5293, Sigma-Aldrich).

Protocols for co-immunoprecipitation, Western blots (Jin et al., 2009), dual-luciferase reporter assay (Jin et al., 2011) were described previously. In the case of luciferase assay, each sample contained three replications. Statistical significance was determined using student's t-test. Results are presented as mean ± standard deviation. All experiments were performed at least three times. Regular immunostaining and Triton X-100 extraction experiments were carried out as described (Wulfkuhle et al., 1999). Prior to fixation, cells were treated with Triton X-100 extraction buffer (0.5% Triton X-100, 50 mM NaCl, 3 mM MgCl2, 30 mM sucrose, 10 mM Pipes, pH 6.8) for 3 minutes at 4°C. After fixation, cells were stained following the standard immunostaining procedure.

RNA extraction, RT-PCR and PCR purification

RNA purification and reverse transcription were performed as described (Rorick et al., 2007). Real-time PCR reactions were performed in triplicate using SYBR green master mix (Applied Biosystems) on an Applied Biosystems 7500 Real-Time PCR System. Values were normalized to the control. Statistical significance was determined by student's t-test. Results are presented as mean±SD. Primers are: Mouse *gli1*, 5'-tccctggtggctttcatcaact-3'; 5'-gcatcattgaaccccgagtaga-3'. Mouse *ptc1*, 5'-gaggctatgtttaatcctcaactc-3'; 5'-ctattatctgatccatgtaacctg-3'. Mouse *β-actin*, 5'-agagggaaatcgtgcgtgac-3'; 5'-caatagtgatgacctggccgt-3'. *Xenopus gli1*, 5'-aagcttcctcacacttgacc-3'; 5'-gctctgcgccatagataatc-3'. *Xenopus ptc1*, 5'-ggacaagaatcgcagagctg-3'; 5'-ggatgctcagggaaccttac-3'. *Xenopus ptc2*, 5'-ccagctcggatctactgagg-3'; 5'-cagtgtctctggatggagca-3'. *Xenopus Hhip*, 5'-gttggtgcaatgcatagtgg-3'; 5'-tcttggttggtggtgtacga-3'. *Xenopus odc*, 5'-gccattgtgaagactctctccattc-3'; 5'-ttcgggtgcttccttgccac-3'. *Xenopus rusc1*, 5'-ggtctgttggttgcgattgg-3'; 5'-acaggcggccgatgttacac-3'. *Xenopus rusc2*, 5'-gacccccttttcatctcttgc-3'; 5'-gtgagatctcttagaagttgggc-3'.

***Xenopus* embryos and manipulations**

Xenopus embryos were obtained as described (Sive et al., 2000). Morpholino antisense oligos used in *Xenopus* experiments are: R1-MO GGTGTCAGTCGTCAGTTACAGCCCC; R1-5mis: GcTGTCAcTCGTCAcTTACAcCCgC; R1-sb: ATACAGAGAGTCACTTACCTGCCCT; R2-MO1: GCTATCCATCATCAGTGGCTTCTTC; and R2-MO2: GGACATTGGTAAATCAGCAAGAGAT. Morpholino against Gli1 was described (Schwend et al., 2013). Microinjection, animal cap assays, in situ hybridization were performed as described (Sive et al., 2000).

Acknowledgements

We thank for Drs. A. Barnekow and A. Liu for expression constructs and cell lines. We greatly appreciate Dr. JP Saint-Jeannet for valuable suggestions, and Drs. P. Klein and I. Bagchi for reading the manuscript.

Author Contributions

Conceived and designed the experiments: ZJ HZ and JY. Performed the experiments: ZJ TS JF ZB JL WM and JY. Analyzed the data: ZJ and JY. Wrote the paper: JY.

Funding:

TS was supported by a National Institutes of Health fellowship F32EY021708. JY is supported in part by National Institutes of Health grants R01GM093217 and R01GM111816.

References

Aavikko, M., Li, S. P., Saarinen, S., Alhopuro, P., Kaasinen, E., Morgunova, E., Li, Y., Vesanen, K., Smith, M. J., Evans, D. G. et al. (2012) 'Loss of SUFU function in familial multiple meningioma', *Am J Hum Genet* 91(3): 520-6.

Amato, M. A., Boy, S. and Perron, M. (2004) 'Hedgehog signaling in vertebrate eye development: a growing puzzle', *Cell Mol Life Sci* 61(7-8): 899-910.

Bayer, M., Fischer, J., Kremerskothen, J., Ossendorf, E., Matanis, T., Konczal, M., Weide, T. and Barnekow, A. (2005) 'Identification and characterization of Iporin as a novel interaction partner for rab1', *BMC Cell Biol* 6(1): 15.

Boehlke, C., Bashkurov, M., Buescher, A., Krick, T., John, A. K., Nitschke, R., Walz, G. and Kuehn, E. W. (2010) 'Differential role of Rab proteins in ciliary trafficking: Rab23 regulates smoothened levels', *J Cell Sci* 123(Pt 9): 1460-7.

Briscoe, J. (2009) 'Making a grade: Sonic Hedgehog signalling and the control of neural cell fate', *Embo J* 28(5): 457-65.

Briscoe, J. and Small, S. (2015) 'Morphogen rules: design principles of gradient-mediated embryo patterning', *Development* 142(23): 3996-4009.

Briscoe, J. and Therond, P. P. (2013) 'The mechanisms of Hedgehog signalling and its roles in development and disease', *Nat Rev Mol Cell Biol* 14(7): 416-29.

Brugieres, L., Pierron, G., Chompret, A., Paillerets, B. B., Di Rocco, F., Varlet, P., Pierre-Kahn, A., Caron, O., Grill, J. and Delattre, O. (2010) 'Incomplete penetrance of the predisposition to medulloblastoma associated with germ-line SUFU mutations', *J Med Genet* 47(2): 142-4.

Chen, M. H., Wilson, C. W., Li, Y. J., Law, K. K., Lu, C. S., Gacayan, R., Zhang, X., Hui, C. C. and Chuang, P. T. (2009) 'Cilium-independent regulation of Gli protein function by Sufu in Hedgehog signaling is evolutionarily conserved', *Genes Dev* 23(16): 1910-28.

Cheung, H. O., Zhang, X., Ribeiro, A., Mo, R., Makino, S., Puviindran, V., Law, K. K., Briscoe, J. and Hui, C. C. (2009) 'The kinesin protein Kif7 is a critical regulator of Gli transcription factors in mammalian hedgehog signaling', *Sci Signal* 2(76): ra29.

Chi, S., Xie, G., Liu, H., Chen, K., Zhang, X., Li, C. and Xie, J. (2012) 'Rab23 negatively regulates Gli1 transcriptional factor in a Su(Fu)-dependent manner', *Cell Signal* 24(6): 1222-8.

Cooper, A. F., Yu, K. P., Brueckner, M., Brailey, L. L., Johnson, L., McGrath, J. M. and Bale, A. E. (2005) 'Cardiac and CNS defects in a mouse with targeted disruption of suppressor of fused', *Development* 132(19): 4407-17.

Ding, Q., Fukami, S., Meng, X., Nishizaki, Y., Zhang, X., Sasaki, H., Dlugosz, A., Nakafuku, M. and Hui, C. (1999) 'Mouse suppressor of fused is a negative regulator of sonic hedgehog signaling and alters the subcellular distribution of Gli1', *Curr Biol* 9(19): 1119-22.

Eggenschwiler, J. T., Bulgakov, O. V., Qin, J., Li, T. and Anderson, K. V. (2006) 'Mouse Rab23 regulates hedgehog signaling from smoothened to Gli proteins', *Dev Biol* 290(1): 1-12.

Eggenschwiler, J. T., Espinoza, E. and Anderson, K. V. (2001) 'Rab23 is an essential negative regulator of the mouse Sonic hedgehog signalling pathway', *Nature* 412(6843): 194-8.

Endoh-Yamagami, S., Evangelista, M., Wilson, D., Wen, X., Theunissen, J. W., Phamluong, K., Davis, M., Scales, S. J., Solloway, M. J., de Sauvage, F. J. et al. (2009) 'The mammalian Cos2 homolog Kif7 plays an essential role in modulating Hh signal transduction during development', *Curr Biol* 19(15): 1320-6.

Evans, T. M., Ferguson, C., Wainwright, B. J., Parton, R. G. and Wicking, C. (2003) 'Rab23, a negative regulator of hedgehog signaling, localizes to the plasma membrane and the endocytic pathway', *Traffic* 4(12): 869-84.
Fukuda, M., Kobayashi, H., Ishibashi, K. and Ohbayashi, N. (2011) 'Genome-wide investigation of the Rab binding activity of RUN domains: development of a novel tool that specifically traps GTP-Rab35', *Cell Struct Funct* 36(2): 155-70.
Han, Y., Shi, Q. and Jiang, J. (2015) 'Multisite interaction with Sufu regulates Ci/Gli activity through distinct mechanisms in Hh signal transduction', *Proc Natl Acad Sci U S A* 112(20): 6383-8.
He, M., Subramanian, R., Bangs, F., Omelchenko, T., Liem, K. F., Jr., Kapoor, T. M. and Anderson, K. V. (2014) 'The kinesin-4 protein Kif7 regulates mammalian Hedgehog signalling by organizing the cilium tip compartment', *Nat Cell Biol* 16(7): 663-72.
Huangfu, D. and Anderson, K. V. (2006) 'Signaling from Smo to Ci/Gli: conservation and divergence of Hedgehog pathways from Drosophila to vertebrates', *Development* 133(1): 3-14.
Hui, C. C. and Angers, S. (2011) 'Gli proteins in development and disease', *Annu Rev Cell Dev Biol* 27: 513-37.
Humke, E. W., Dorn, K. V., Milenkovic, L., Scott, M. P. and Rohatgi, R. (2010) 'The output of Hedgehog signaling is controlled by the dynamic association between Suppressor of Fused and the Gli proteins', *Genes Dev* 24(7): 670-82.
Jia, J. and Jiang, J. (2006) 'Decoding the Hedgehog signal in animal development', *Cell Mol Life Sci* 63(11): 1249-65.
Jia, J., Kolterud, A., Zeng, H., Hoover, A., Teglund, S., Toftgard, R. and Liu, A. (2009) 'Suppressor of Fused inhibits mammalian Hedgehog signaling in the absence of cilia', *Dev Biol* 330(2): 452-60.
Jiang, J. and Hui, C. C. (2008) 'Hedgehog signaling in development and cancer', *Dev Cell* 15(6): 801-12.
Jin, Z., Mei, W., Strack, S., Jia, J. and Yang, J. (2011) 'The antagonistic action of B56-containing protein phosphatase 2As and casein kinase 2 controls the phosphorylation and Gli turnover function of Daz interacting protein 1', *J Biol Chem* 286(42): 36171-9.
Jin, Z., Shi, J., Saraf, A., Mei, W., Zhu, G. Z., Strack, S. and Yang, J. (2009) 'The 48-kDa alternative translation isoform of PP2A:B56epsilon is required for Wnt signaling during midbrain-hindbrain boundary formation', *J Biol Chem* 284(11): 7190-200.
Jin, Z., Wallace, L., Harper, S. Q. and Yang, J. (2010) 'PP2A:B56{epsilon}, a substrate of caspase-3, regulates p53-dependent and p53-independent apoptosis during development', *J Biol Chem* 285(45): 34493-502.
Kijima, C., Miyashita, T., Suzuki, M., Oka, H. and Fujii, K. (2012) 'Two cases of nevoid basal cell carcinoma syndrome associated with meningioma caused by a PTCH1 or SUFU germline mutation', *Fam Cancer* 11(4): 565-70.
Kogerman, P., Grimm, T., Kogerman, L., Krause, D., Unden, A. B., Sandstedt, B., Toftgard, R. and Zaphiropoulos, P. G. (1999) 'Mammalian suppressor-of-fused modulates nuclear-cytoplasmic shuttling of Gli-1', *Nat Cell Biol* 1(5): 312-9.
Koide, T., Hayata, T. and Cho, K. W. (2006) 'Negative regulation of Hedgehog signaling by the cholesterogenic enzyme 7-dehydrocholesterol reductase', *Development* 133(12): 2395-405.
Law, K. K., Makino, S., Mo, R., Zhang, X., Puviindran, V. and Hui, C. C. (2012) 'Antagonistic and cooperative actions of Kif7 and Sufu define graded intracellular Gli activities in Hedgehog signaling', *PLoS ONE* 7(11): e50193.

Lee, J., Platt, K. A., Censullo, P. and Ruiz i Altaba, A. (1997) 'Gli1 is a target of Sonic hedgehog that induces ventral neural tube development', *Development* 124(13): 2537-52.
Li, N., Volff, J. N. and Wizenmann, A. (2007) 'Rab23 GTPase is expressed asymmetrically in Hensen's node and plays a role in the dorsoventral patterning of the chick neural tube', *Dev Dyn* 236(11): 2993-3006.
Li, Z. J., Nieuwenhuis, E., Nien, W., Zhang, X., Zhang, J., Puviindran, V., Wainwright, B. J., Kim, P. C. and Hui, C. C. (2012) 'Kif7 regulates Gli2 through Sufu-dependent and -independent functions during skin development and tumorigenesis', *Development* 139(22): 4152-61.
Liem, K. F., Jr., He, M., Ocbina, P. J. and Anderson, K. V. (2009) 'Mouse Kif7/Costal2 is a cilia-associated protein that regulates Sonic hedgehog signaling', *Proc Natl Acad Sci U S A* 106(32): 13377-82.
Lin, C., Yao, E., Wang, K., Nozawa, Y., Shimizu, H., Johnson, J. R., Chen, J. N., Krogan, N. J. and Chuang, P. T. (2014) 'Regulation of Sufu activity by p66beta and Mycbp provides new insight into vertebrate Hedgehog signaling', *Genes Dev* 28(22): 2547-63.
Liu, J., Heydeck, W., Zeng, H. and Liu, A. (2012) 'Dual function of suppressor of fused in Hh pathway activation and mouse spinal cord patterning', *Dev Biol* 362(2): 141-53.
Lupo, G., Harris, W. A. and Lewis, K. E. (2006) 'Mechanisms of ventral patterning in the vertebrate nervous system', *Nat Rev Neurosci* 7(2): 103-14.
MacDonald, J. I., Dietrich, A., Gamble, S., Hryciw, T., Grant, R. I. and Meakin, S. O. (2012) 'Nesca, a novel neuronal adapter protein, links the molecular motor kinesin with the pre-synaptic membrane protein, syntaxin-1, in hippocampal neurons', *J Neurochem* 121(6): 861-80.
Maurya, A. K., Ben, J., Zhao, Z., Lee, R. T., Niah, W., Ng, A. S., Iyu, A., Yu, W., Elworthy, S., van Eeden, F. J. et al. (2013) 'Positive and negative regulation of Gli activity by Kif7 in the zebrafish embryo', *PLoS Genet* 9(12): e1003955.
Min, T. H., Kriebel, M., Hou, S. and Pera, E. M. (2011) 'The dual regulator Sufu integrates Hedgehog and Wnt signals in the early Xenopus embryo', *Dev Biol* 358(1): 262-76.
Moody, S. A. (1987) 'Fates of the blastomeres of the 16-cell stage Xenopus embryo', *Dev Biol* 119(2): 560-78.
Moody, S. A. (2012) 'Testing retina fate commitment in Xenopus by blastomere deletion, transplantation, and explant culture', *Methods Mol Biol* 884: 115-27.
Murcia, N. S., Richards, W. G., Yoder, B. K., Mucenski, M. L., Dunlap, J. R. and Woychik, R. P. (2000) 'The Oak Ridge Polycystic Kidney (orpk) disease gene is required for left-right axis determination', *Development* 127(11): 2347-55.
Murone, M., Luoh, S. M., Stone, D., Li, W., Gurney, A., Armanini, M., Grey, C., Rosenthal, A. and de Sauvage, F. J. (2000) 'Gli regulation by the opposing activities of fused and suppressor of fused', *Nat Cell Biol* 2(5): 310-2.
Mussolino, C., Morbitzer, R., Lutge, F., Dannemann, N., Lahaye, T. and Cathomen, T. (2011) 'A novel TALE nuclease scaffold enables high genome editing activity in combination with low toxicity', *Nucleic Acids Res* 39(21): 9283-93.
Nguyen, V., Chokas, A. L., Stecca, B. and Ruiz i Altaba, A. (2005) 'Cooperative requirement of the Gli proteins in neurogenesis', *Development* 132(14): 3267-79.
Pastorino, L., Ghiorzo, P., Nasti, S., Battistuzzi, L., Cusano, R., Marzocchi, C., Garre, M. L., Clementi, M. and Scarra, G. B. (2009) 'Identification of a SUFU germline mutation in a family with Gorlin syndrome', *Am J Med Genet A* 149A(7): 1539-43.

Pearse, R. V., 2nd, Collier, L. S., Scott, M. P. and Tabin, C. J. (1999) 'Vertebrate homologs of Drosophila suppressor of fused interact with the gli family of transcriptional regulators', *Dev Biol* 212(2): 323-36.
Petrova, R. and Joyner, A. L. (2014) 'Roles for Hedgehog signaling in adult organ homeostasis and repair', *Development* 141(18): 3445-57.
Preat, T. (1992) 'Characterization of Suppressor of fused, a complete suppressor of the fused segment polarity gene of Drosophila melanogaster', *Genetics* 132(3): 725-36.
Rorick, A. M., Mei, W., Liette, N. L., Phiel, C., El-Hodiri, H. M. and Yang, J. (2007) 'PP2A:B56epsilon is required for eye induction and eye field separation', *Dev Biol* 302(2): 477-493.
Sasaki, H., Hui, C., Nakafuku, M. and Kondoh, H. (1997) 'A binding site for Gli proteins is essential for HNF-3beta floor plate enhancer activity in transgenics and can respond to Shh in vitro', *Development* 124(7): 1313-22.
Schulman, J. M., Oh, D. H., Sanborn, J. Z., Pincus, L., McCalmont, T. H. and Cho, R. J. (2015) 'Multiple Hereditary Infundibulocystic Basal Cell Carcinoma Syndrome Associated With a Germline SUFU Mutation', *JAMA Dermatol*: 1-5.
Schwend, T., Jin, Z., Jiang, K., Mitchell, B. J., Jia, J. and Yang, J. (2013) 'Stabilization of speckle-type POZ protein (Spop) by Daz interacting protein 1 (Dzip1) is essential for Gli turnover and the proper output of Hedgehog signaling', *J Biol Chem* 288(45): 32809-20.
Sive, H., Grainger, R. and Harland, R. (2000) *Early Development of Xenopus laevis; A Laboratory Manual*, Cold Spring Harbor: Cold Spring Harbor Press.
Stone, D. M., Murone, M., Luoh, S., Ye, W., Armanini, M. P., Gurney, A., Phillips, H., Brush, J., Goddard, A., de Sauvage, F. J. et al. (1999) 'Characterization of the human suppressor of fused, a negative regulator of the zinc-finger transcription factor Gli', *J Cell Sci* 112 (Pt 23): 4437-48.
Sun, Q., Han, C., Liu, L., Wang, Y., Deng, H., Bai, L. and Jiang, T. (2012) 'Crystal structure and functional implication of the RUN domain of human NESCA', *Protein Cell* 3(8): 609-17.
Svard, J., Heby-Henricson, K., Persson-Lek, M., Rozell, B., Lauth, M., Bergstrom, A., Ericson, J., Toftgard, R. and Teglund, S. (2006) 'Genetic elimination of Suppressor of fused reveals an essential repressor function in the mammalian Hedgehog signaling pathway', *Dev Cell* 10(2): 187-97.
Tay, S. Y., Ingham, P. W. and Roy, S. (2005) 'A homologue of the Drosophila kinesin-like protein Costal2 regulates Hedgehog signal transduction in the vertebrate embryo', *Development* 132(4): 625-34.
Taylor, M. D., Liu, L., Raffel, C., Hui, C. C., Mainprize, T. G., Zhang, X., Agatep, R., Chiappa, S., Gao, L., Lowrance, A. et al. (2002) 'Mutations in SUFU predispose to medulloblastoma', *Nat Genet* 31(3): 306-10.
Tukachinsky, H., Lopez, L. V. and Salic, A. (2010) 'A mechanism for vertebrate Hedgehog signaling: recruitment to cilia and dissociation of SuFu-Gli protein complexes', *J Cell Biol* 191(2): 415-28.
Wang, C., Pan, Y. and Wang, B. (2010) 'Suppressor of fused and Spop regulate the stability, processing and function of Gli2 and Gli3 full-length activators but not their repressors', *Development* 137(12): 2001-9.
Wilson, C. W. and Chuang, P. T. (2010) 'Mechanism and evolution of cytosolic Hedgehog signal transduction', *Development* 137(13): 2079-94.
Wolff, C., Roy, S. and Ingham, P. W. (2003) 'Multiple muscle cell identities induced by distinct levels and timing of hedgehog activity in the zebrafish embryo', *Curr Biol* 13(14): 1169-81.

Wulfkuhle, J. D., Donina, I. E., Stark, N. H., Pope, R. K., Pestonjamasp, K. N., Niswonger, M. L. and Luna, E. J. (1999) 'Domain analysis of supervillin, an F-actin bundling plasma membrane protein with functional nuclear localization signals', *J Cell Sci* 112 (Pt 13): 2125-36.
Zeng, H., Jia, J. and Liu, A. (2010) 'Coordinated translocation of mammalian Gli proteins and suppressor of fused to the primary cilium', *PLoS ONE* 5(12): e15900.
Zhang, Q., Shi, Q., Chen, Y., Yue, T., Li, S., Wang, B. and Jiang, J. (2009) 'Multiple Ser/Thr-rich degrons mediate the degradation of Ci/Gli by the Cul3-HIB/SPOP E3 ubiquitin ligase', *Proc Natl Acad Sci U S A* 106(50): 21191-6.
Zhang, Q., Zhang, L., Wang, B., Ou, C. Y., Chien, C. T. and Jiang, J. (2006) 'A hedgehog-induced BTB protein modulates hedgehog signaling by degrading Ci/Gli transcription factor', *Dev Cell* 10(6): 719-29.
Zhang, Y., Fu, L., Qi, X., Zhang, Z., Xia, Y., Jia, J., Jiang, J., Zhao, Y. and Wu, G. (2013) 'Structural insight into the mutual recognition and regulation between Suppressor of Fused and Gli/Ci', *Nat Commun* 4: 2608.

Figures

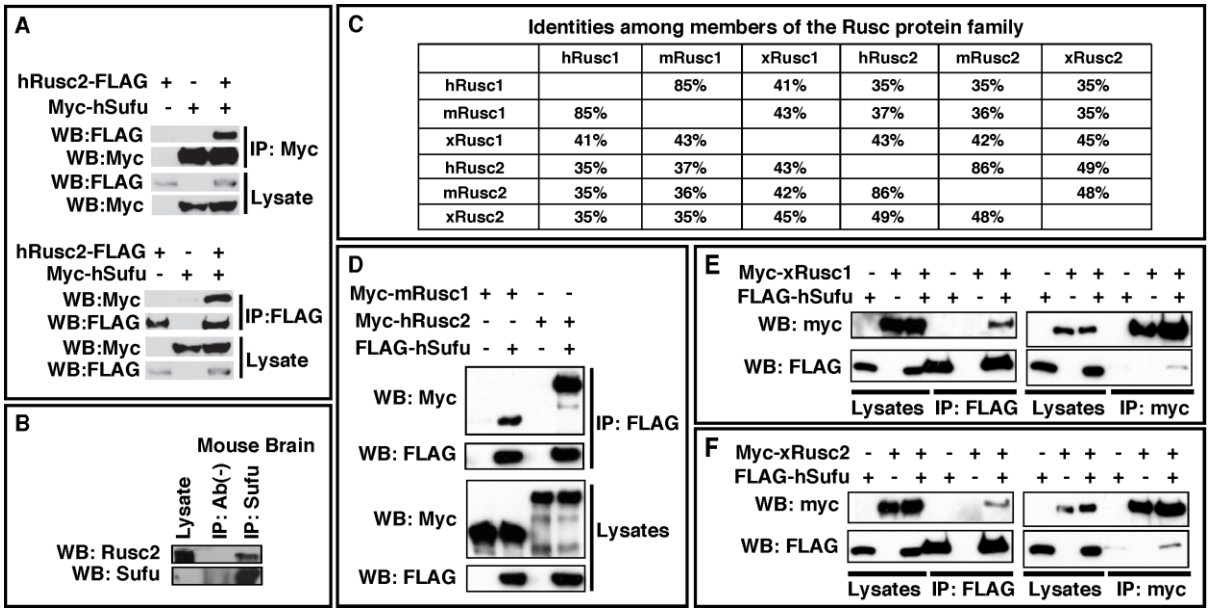

	hRusc1	mRusc1	xRusc1	hRusc2	mRusc2	xRusc2
hRusc1		85%	41%	35%	35%	35%
mRusc1	85%		43%	37%	36%	35%
xRusc1	41%	43%		43%	42%	45%
hRusc2	35%	37%	43%		86%	49%
mRusc2	35%	36%	42%	86%		48%
xRusc2	35%	35%	45%	49%	48%	

Figure 1. Members of the Rusc protein family interact with Sufu. A. Coimmunoprecipitation (CoIP) showing the interaction between hSufu and hRusc2. hRusc2-FLAG and myc-hSufu were expressed in HEK293T cells alone or in combination. CoIP was performed using an anti-myc antibody (upper panel) or an anti-FLAG antibody (lower panel). **B**. CoIP showing endogenous Sufu and Rusc2 formed a complex in mouse whole brain lysate. Sufu was immunoprecipitated. **C.** Identity between the Rusc proteins. Protein sequences of Rusc1 and Rusc2 from human, mouse, and *Xenopus* were aligned using the NCBI online blast tool (http://blast.ncbi.nlm.nih.gov/Blast.cgi?PAGE_TYPE=BlastSearch&BLAST_SPEC=blast2seq&LINK_LOC=align2seq). **D**. CoIP results to show that mRusc1 and hRusc2 formed complexes with hSufu. **E**. CoIP showing that myc-xRusc1 interacted with FLAG-hSufu. **F**. CoIP showing that myc-xRusc2 interacted with FLAG-hSufu.

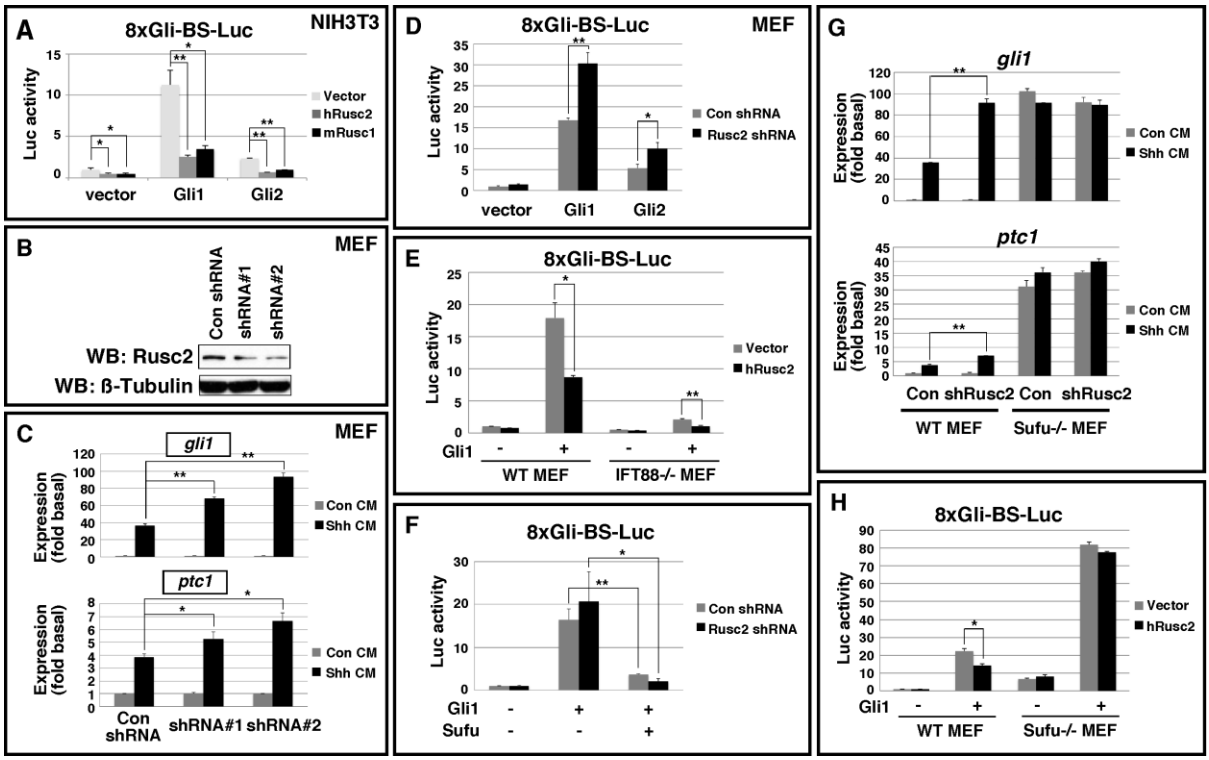

Figure 2. Rusc proteins inhibit Hh signaling. A. Dual-luciferase assay showing that mRusc1 and hRusc2 inhibited the activities of Gli1 and Gli2 in the 8xGli-BS-Luciferase reporter assay. **B**. Western blot showing reduced expression of Rusc2 in MEFs infected with lentiviral shRNAs against Rusc2. **C**. Real-time RT-PCR results showing that Shh-N conditioned medium induced the expression of *gli1* and *ptc1* in MEFs. Knockdown of Rusc2 by lentiviral shRNAs enhanced the activity of Shh-N conditioned medium in this assay. The expression level of *gli1* and *ptc1* was normalized to that of *ß-actin*. **D**. Dual-luciferase assay showing that knockdown of Rusc2 in MEFs enhanced the activities of Gli1 and Gli2. **E**. Dual-luciferase assay showing that overexpression of hRusc2 reduced the activity of Gli1 in wild type MEFs and IFT88 knockout (IFT88-/-) MEFs. **F**. Dual-luciferase assay showing that overexpression of hSufu reduced the activity of Gli1 in control and Rusc2 knockdown MEFs. **G**. Real-time RT-PCR results showing that knockdown of Rusc2 increased the expression of *gli1* and *ptc1* induced by Shh-N conditioned medium in wild type MEFs. In Sufu knockout MEFs, knockdown of Rusc2 had no effect on the expression of *gli1* and *ptc1*. **H**. Dual-luciferase assay showing that overexpression of Rusc2 in wild type MEFs, but not Sufu knockout MEFs, reduced the activity of Gli1 in the 8xGli-BS-Luciferase reporter assay. In **A**, **C-H**, data is shown as mean±SD. *p<0.05, **p<0.01.

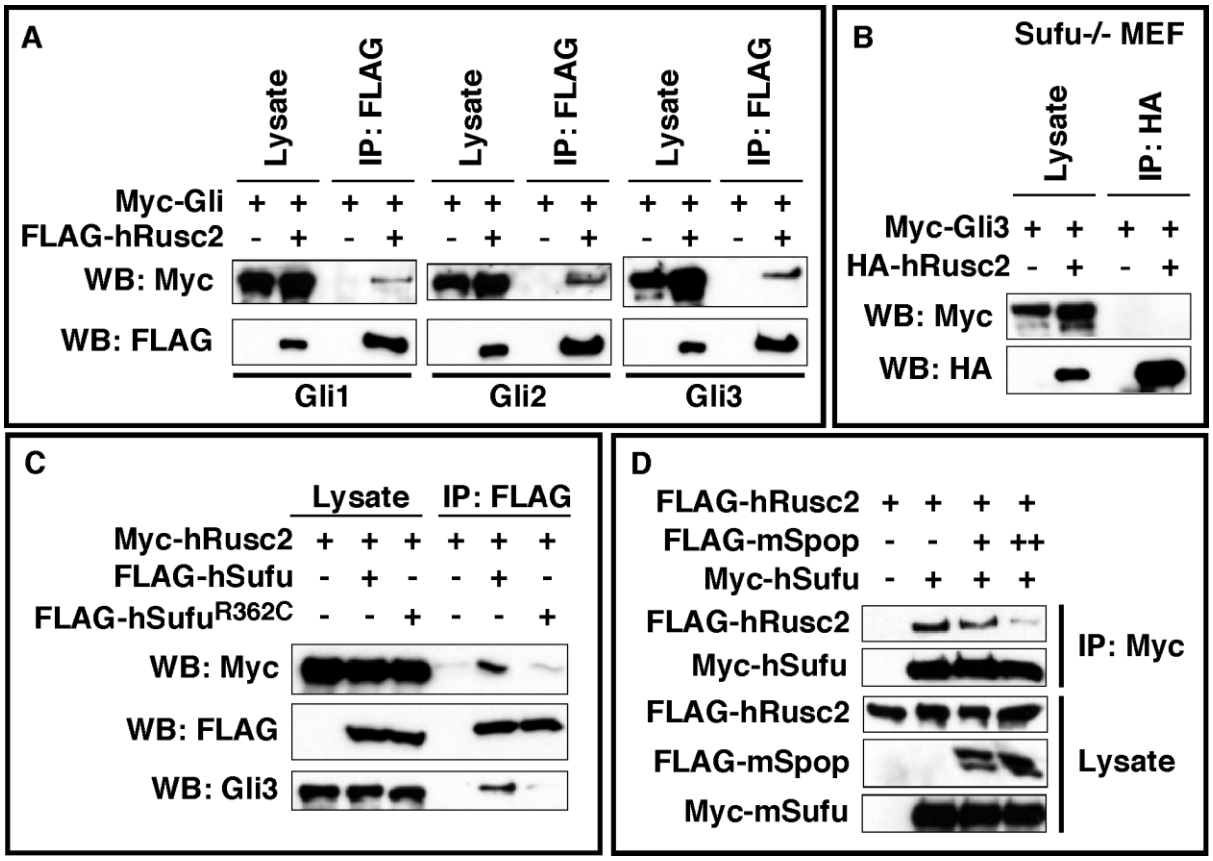

Figure 3. Rusc2 forms a heterotrimeric complex with Sufu and Gli proteins. A. CoIP showing that FLAG-hRusc2 interacted with myc-Gli1 (left panel), myc-Gli2 (middle panel), and myc-Gli3 (right panel). **B**. CoIP showing lack of complex formation between overexpressed Rusc2 and Gli3 in Sufu knockout MEFs. **C**. CoIP showing that hRusc2 formed a complex with the wild type hSufu, but not hSufu^{R362C}, which is deficient in binding Gli protein. **D**. CoIP showing that overexpression of mSpop reduced the interaction between hSufu and hRusc2.

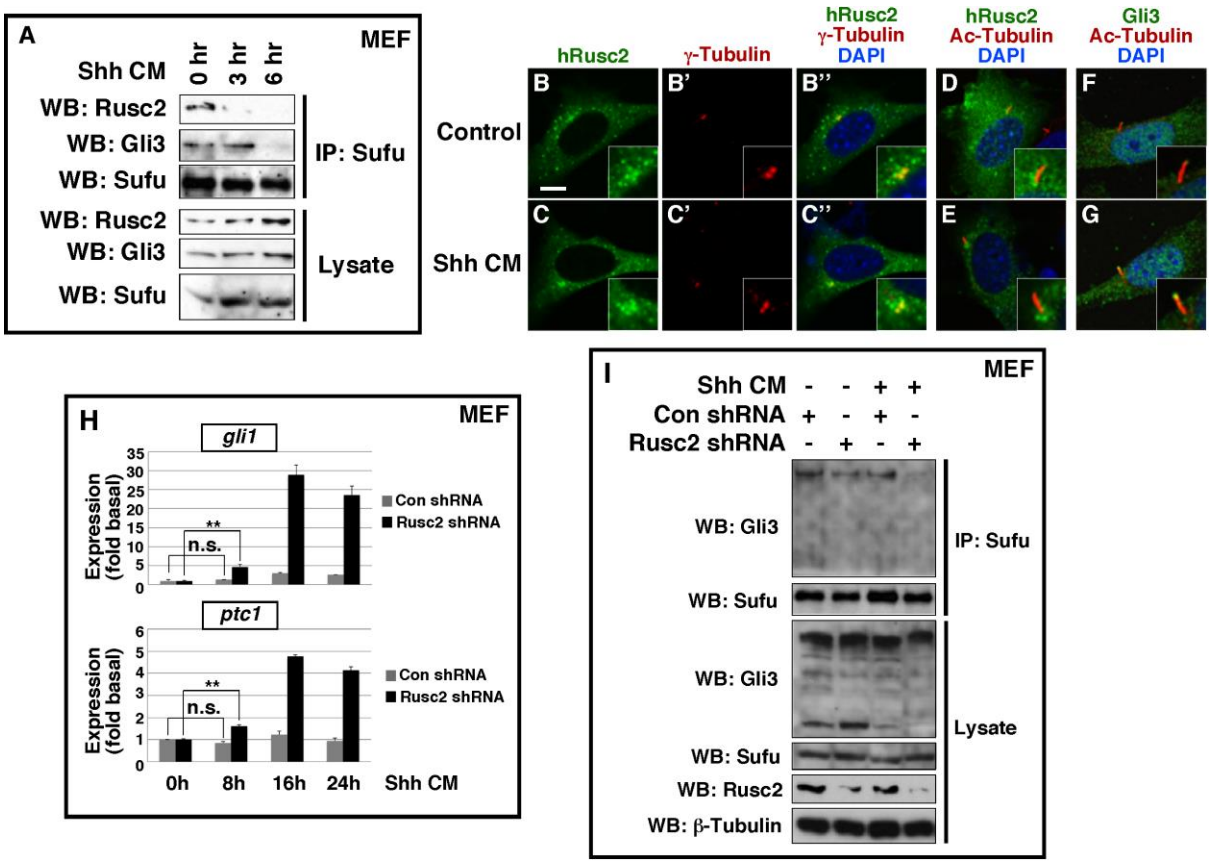

Figure 4. Rusc2 inhibits signaling-induced dissociation of the Sufu-Gli protein complexes. A. CoIP showing sequential dissociation of the Rusc2-Sufu-Gli3 complexes in MEFs upon Shh-conditioned medium treatment. Endogenous Sufu was immunoprecipitated. The amount of endogenous Gli3 and Rusc2 associated with Sufu was assessed by Western blot. **B-G**. Confocal images to show the subcellular localization of FLAG-hRucs2 in control (upper panels) and Shh conditioned medium stimulated (lower panels) cells. **B** and **C** are anti-FLAG staining (Rusc2). **B'** and **C'** are γ-Tubulin staining. **B"** is a merged image of **B** and **B'**. **C"** is a merged image of **C** and **C'**. **D** and **E** are merged images of hRusc2 and acetylated-Tubulin double staining. **F** and **G** are merged images of Gli3 and acetylated-Tubulin double staining. Boxed images in the lower-right corner of each panel are higher magnification views of the area around cilia. Scale bars: 10 μm. **H.** Real-time RT-PCR showing the expression of *gli1* and *ptc1* in un-stimulated MEFs and MEFs treated with Shh-N conditioned medium for 8, 16, and 24 hours. Data is shown as mean±SD. **p<0.01. n.s., non-significant. **I**. CoIP experiments to assess the effect of Rusc2 knockdown on Shh-induced dissociation of the Sufu-Gli3 protein complexes in MEFs. Endogenous Sufu and Gli3 were analyzed. The dose of Shh-N conditioned medium used in this experiment was identical as that in **H**.

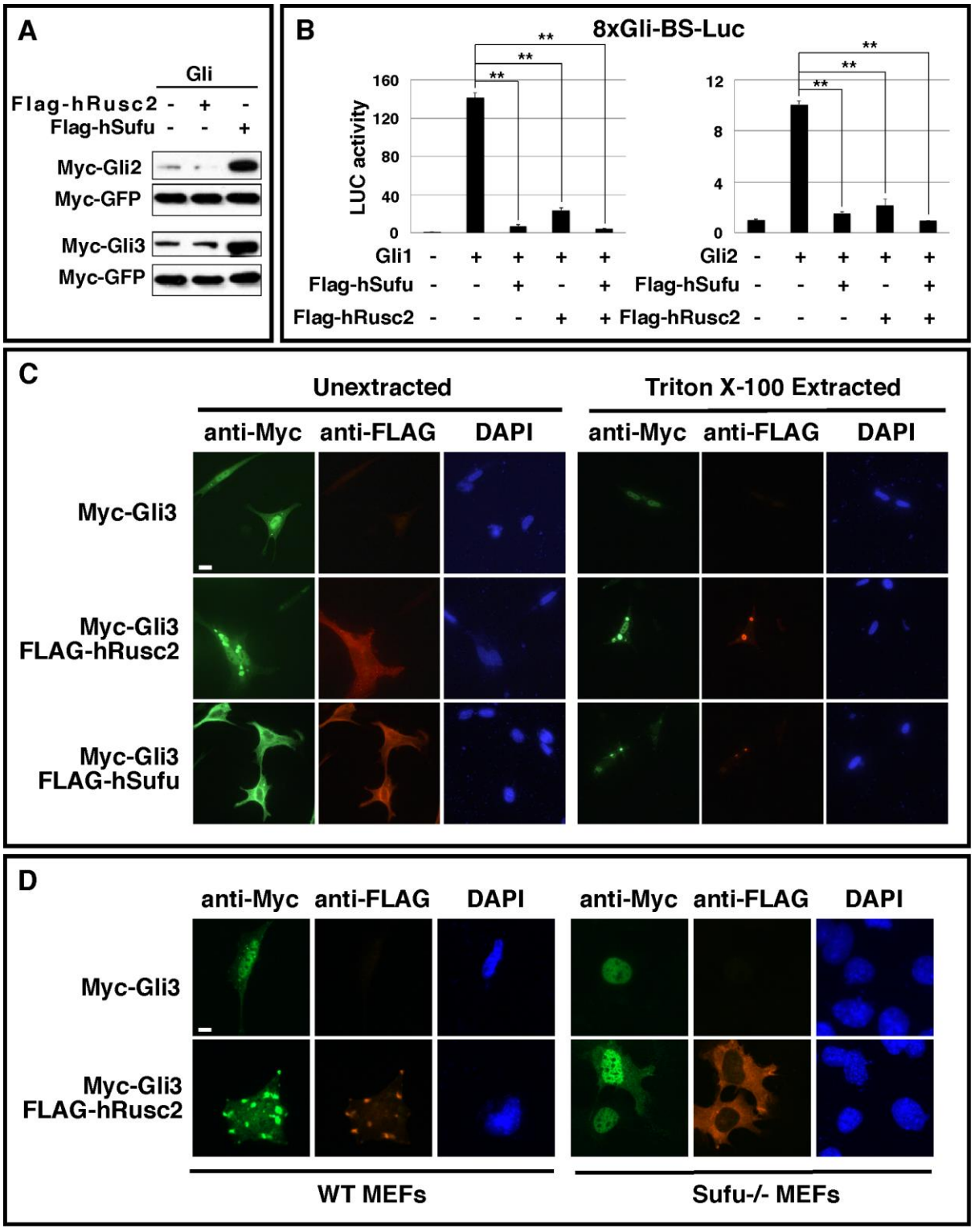

Figure 5. Rusc2 induces cytosolic Gli protein aggregates. A. Western blot showing that overexpression of hSufu, but not hRusc2, stabilized Gli2 and Gli3 in NIH3T3 cells. **B**. Dual-luciferase assay showing that hSufu and hRusc2 reduced the activity of Gli1 and Gli2. Compared to hSufu, hRusc2 was less potent in this assay. Data is shown as mean±SD.

p<0.01. **C. Immunofluorescence showing the effects of hSufu and hRusc2 on the subcellular localization of myc-Gli3 in NIH3T3 cells. Left panels are cells without Triton X-100 extraction. Right panels are cell extracted with Triton X-100 prior to fixation. Scale bars: 10 μm. **D**. Immunofluorescence showing that overexpression of hRusc2 altered the subcellular distribution of myc-Gli3 in wild type MEFs (left), but not that in Sufu knockout MEFs (right). Scale bars: 10 μm.

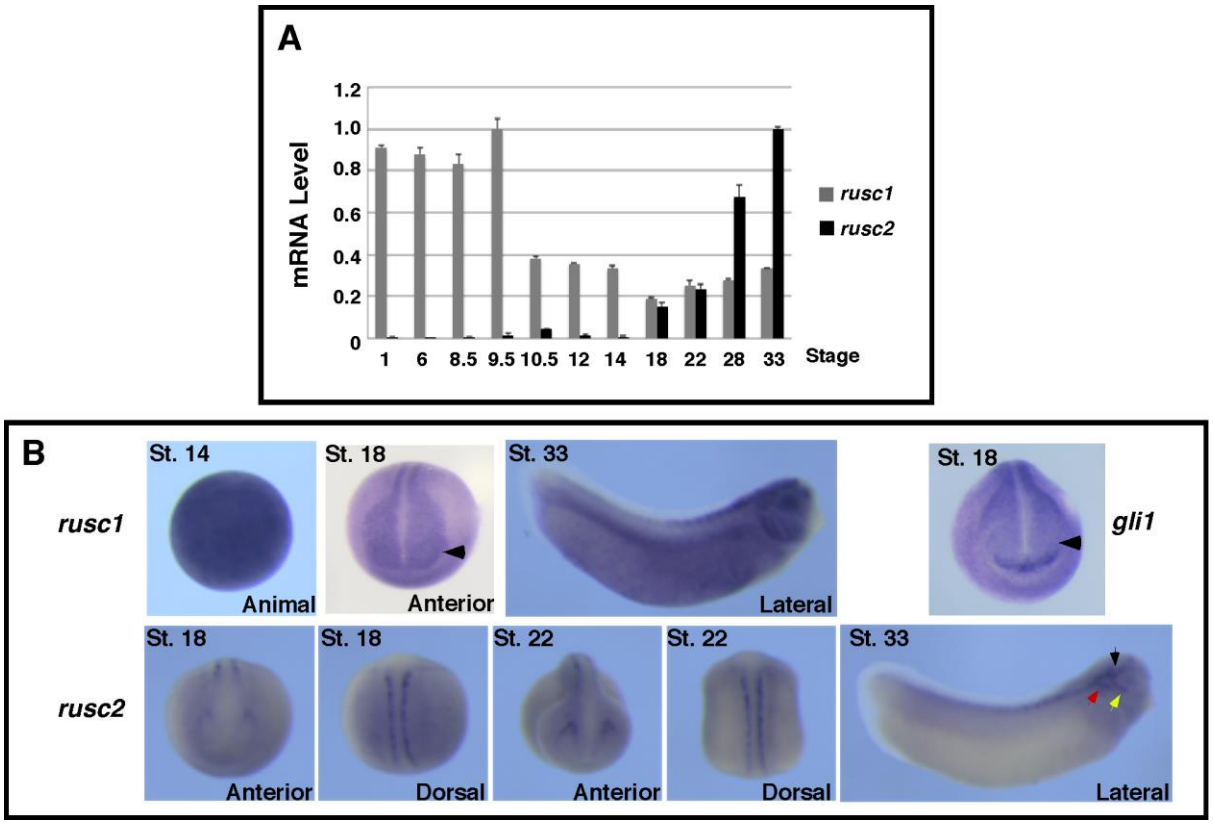

Figure 6. Expression of *rusc1* and *rusc2* during *Xenopus* eye development. A. Real-time RT-PCR showing the temporal expression of *rusc1* and *rusc2* during *Xenopus* development. The expression level of *rusc1* and *rusc2* was normalized to that of *odc*. Data is shown as mean±SD. **B**. Whole mount in situ hybridization showing the spatial expression pattern of *rusc1*, *rusc2*, and *gli1*. St.: stage. Arrowheads point to the eye domains, which express *rusc1*, but not *gli1*. Black, red, and yellow arrows pointed to the trigeminal ganglion, middle lateral line placode, and anterodorsal lateral line placode, respectively.

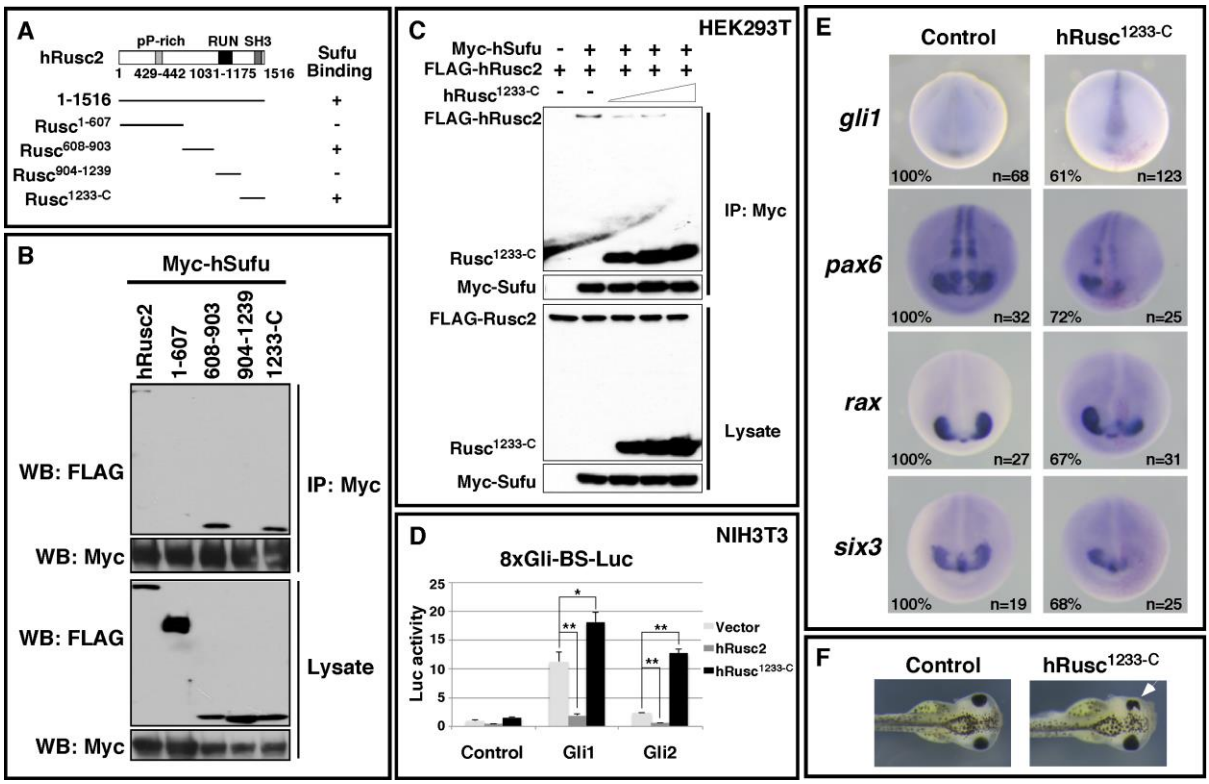

Figure 7. Dominant negative Rusc enhances Hh signaling in *Xenopus* embryos and impairs eye development. A. Schematic diagram of hRusc2 and deletion constructs. Whether a Rusc2 construct interacts with hSufu in the CoIP experiment is summarized by "+" (interaction detected) or "-" (interaction not detected). **B**. CoIP results showing that hSufu interacted with the full-length hRusc2, Rusc$^{608\text{-}903}$, and Rusc$^{1233\text{-}C}$. **C**. CoIP results showing that overexpression of Rusc$^{1233\text{-}C}$ reduced the binding between hSufu and the full-length hRusc2. **D**. Dual-luciferase assay showing that the activities of Gli1 and Gli2 were enhanced by co-overexpression of Rusc$^{1233\text{-}C}$ in NIH3T3 cells. Data is shown as mean±SD. *p<0.05, **p<0.01. **E**. In situ hybridization showing the expression of *gli1*, *pax6*, *rax*, and *six3* in control (left panels) and Rusc$^{1233\text{-}C}$ overexpressed (right panels) embryos at stage 20. At the 8-cell stage, one of the dorsal animal blastomeres was injected with a mixture of Rusc$^{1233\text{-}C}$ (1 ng) and n-ß-gal (250 pg) RNAs. **F**. Overexpression of Rusc$^{1233\text{-}C}$ (1 ng) reduced the size of the eye (pointed by the arrow).

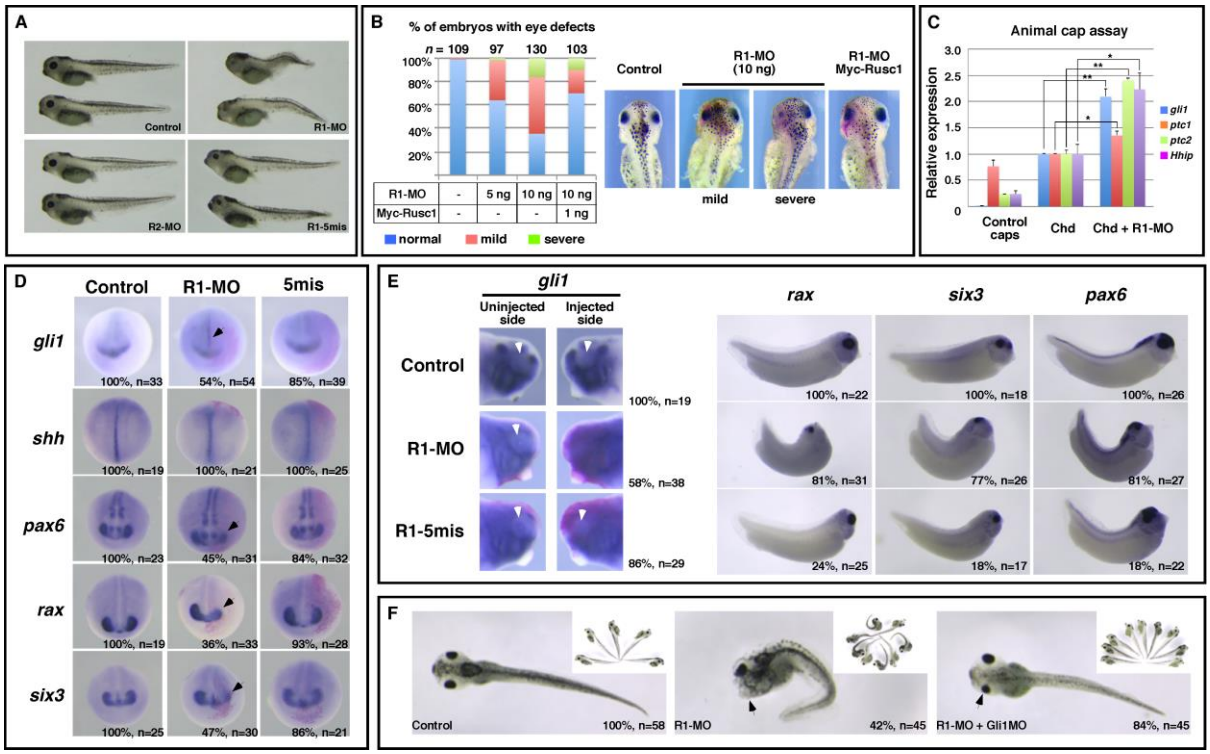

Figure 8. Rusc1 inhibits Hh signaling during *Xenopus* eye development. A. Whole embryo morphology of uninjected embryos, and embryos injected with R1-MO, R1-5mis, and R2-MO. Morpholinos (20 ng) were injected into both dorsal blastomeres at the 4-cell stage. **B**. Overexpression of myc-xRusc1 rescued phenotypes induced by unilateral injection of R1-MO. Left panel is a summary of embryos with eye defect. Images in the right panel are representative embryos. A 50% or greater reduction in the size of the eye is considered as "severe". A reduction less than 50% in the eye size is considered as "mild". **C**. Real-time RT-PCR showing the expression of *gli1*, *ptc1*, *ptc2*, and *Hhip* in animal caps. Chordin (Chd, 25 pg) was injected into the animal pole of control and R1-MO (40 ng) injected embryos at the 1-cell stage. Animal caps were dissected at the late blastula stage and harvested at stage 22. Data is shown as mean±SD. *p<0.05, **p<0.01. **D**. In situ hybridization showing that unilateral injection of R1-MO (20 ng) enhanced the expression of *gli1*, and reduced the expression of *pax6*, *rax*, and *six3*. The expression of *shh* was not altered by R1-MO injection. Embryos were analyzed at stage 20. **E**. In situ hybridization showing that unilateral injection of R1-MO enhanced the expression of *gli1* in the head region and reduced the expression of *pax6*, *rax*, and *six3* at stage 33. **F**. Morphology of uninjected embryos, embryos unilaterally injected with R1-MO alone or R1-MO together with Gli1 morpholino (Gli1MO). Arrows in **D** and **F** point to the developing eyes.

Supplemental Figures

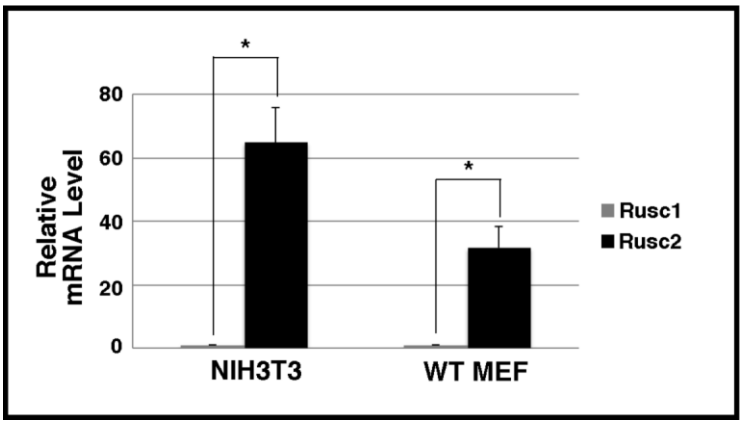

Supplemental Figure 1.

Expression of *rusc1* and *rusc2* in MEFs and NIH3T3 cells. Real-time RT-PCR showing that *rusc2*, but not *rusc1*, is abundantly expressed in NIH3T3 and MEFs. In the real-time PCR experiment, pCS2-Rusc1 and pCS2-Rusc2 plasmids (0.4 pg) were used as the control for normalization. Data are shown as mean±SD. *$p<0.05$.

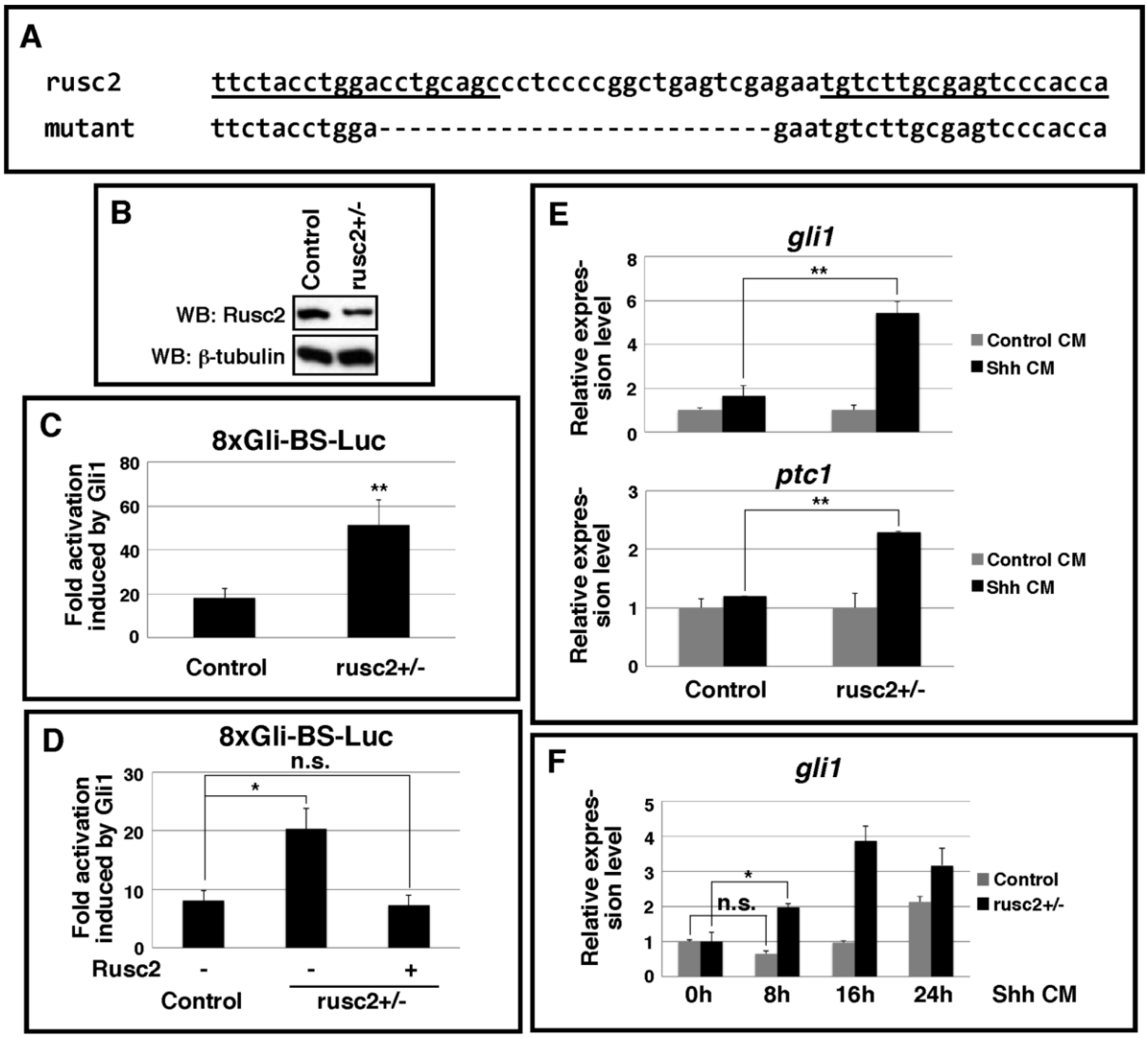

Supplemental Figure 2.

Enhanced Hh response in rusc2 heterozygous mutant MEFs. A. Schematic diagram showing the sequences of the wild type and mutant rusc2 alleles. Sequences targeted by the left and right TALEN arms are underlined. To establish rusc2 mutant cell lines, wild type MEFs were transfected with TALEN and selected by puromycin. Several cell lines were established from TALEN-transfected single cells. The targeted loci of these cells were sequenced. A cell line carrying a mutated rusc2 allele was identified. When testing the Hh response of this rusc2 heterozygous mutant MEF cell line, we used an un-mutated MEF cell line established through the same procedure as the control. **B.** Western blot to show that the expression of Rusc2 is reduced in rusc2 heterozygous mutant MEFs. **C.** Dual-luciferase assay showing that transfection of Gli1 (100 ng) into control MEFs activated the 8xGli-BS-Luciferase reporter by 19 folds. In the rusc2 heterozygous mutant MEFs, the

same amount of Gli1 activated the 8xGli-BS-Luciferase reporter by 51 folds. Data is shown as mean±SD. **p<0.01. **D.** Overexpression of FLAG-hRusc2 rescued the response of the rusc2 heterozygous mutant MEFs to Gli1 in an 8xGli-BS-Luciferase reporter assay. Data is shown as mean±SD. *p<0.05, n.s., non-significant. **E**. Real-time RT-PCR results showing that a low dose of Shh-conditioned medium, which was insufficient for activating *gli1* and *ptc1* expression in control MEFs, markedly increased the expression of *gli1* and *ptc1* in rusc2 heterozygous mutant MEFs. Data is shown as mean±SD. **p<0.01. **F**. Real-time RT-PCR results showing the expression of *gli1* in control and rusc2 heterozygous mutant MEFs at various time points after Shh conditioned medium treatment. Compared to control MEFs, rusc2 heterozygous mutant MEFs showed accelerated *gli1* activation kinetics in response to Shh conditioned medium treatment. Data is shown as mean±SD. *p<0.05, n.s., non-significant.

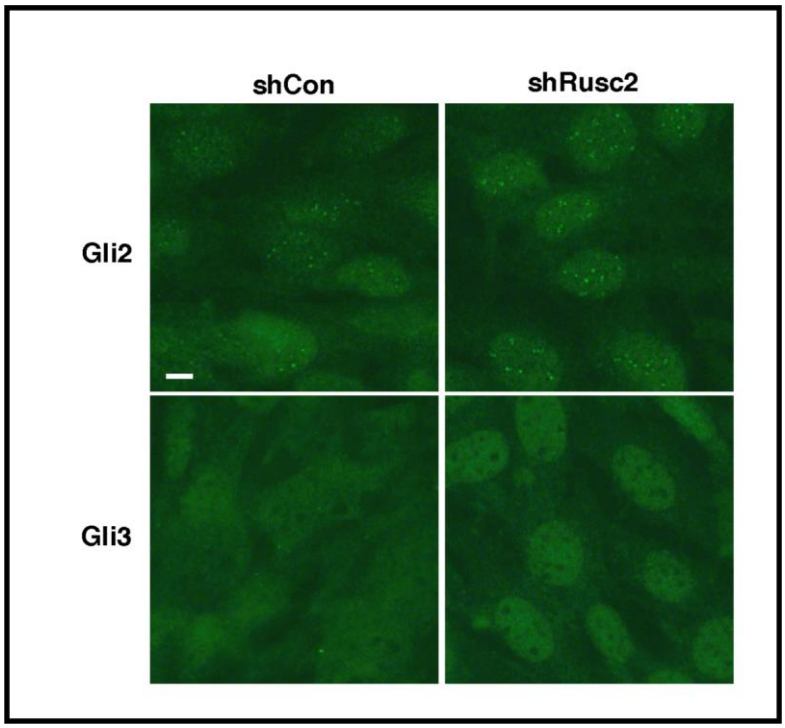

Supplemental Figure 3.

Knockdown of rusc2 does not significantly alter the subcellular localization of endogenous Gli2 and Gli3. Immunofluorescence showing subcellular localization of endogenous Gli2 (upper panels) and Gli3 (lower panels) in control shRNA (left) and Rusc2 shRNA infected cells. Scale bars: 10μm.

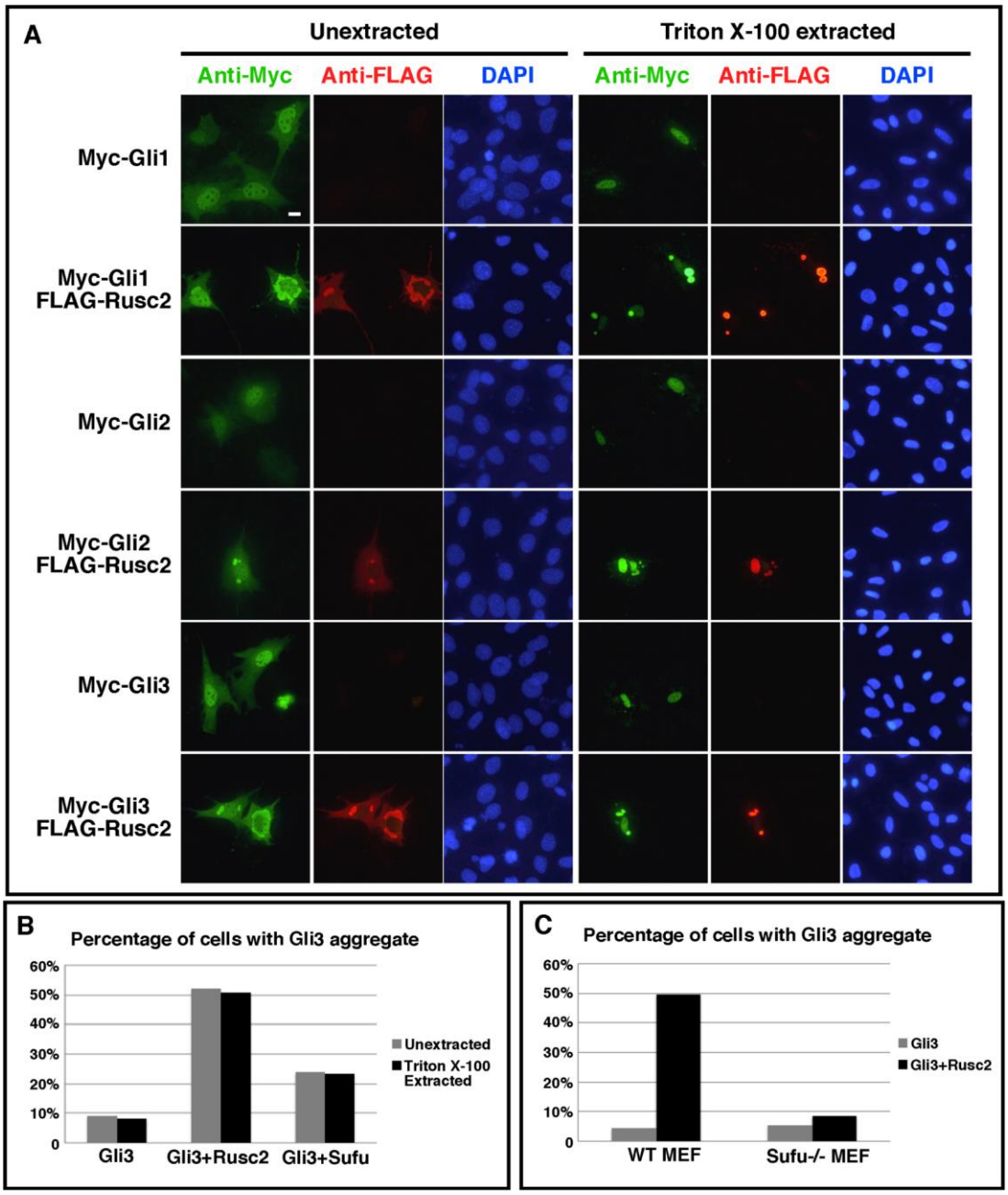

Supplemental Figure 4.

Overexpression of rusc2 induces cytoplasmic Gli1, Gli2, and Gli3 protein aggregates, which are resistant to Triton X-100 extraction. A. Immunofluorescence showing that overexpression of Rusc2 altered the subcellular distribution of myc-Gli1, myc-Gli2, and myc-Gli3 in NIH3T3 cells. When expressed alone, Gli proteins were enriched in the nucleus. Overexpression of hRusc2 decreased the amount of Gli proteins in the nucleus and induced cytoplasmic Gli protein aggregates. In the Triton extraction experiment, cells were pre-extracted with 0.5% Triton X-100 in a cytoskeleton stabilizing buffer for 3 minutes at 4°C

prior to fixation. This treatment condition was sufficient for removing all cytosolic GFP in myc-GFP transfected cells (not shown). However, Gli protein aggregates remained in the cytoplasm after cells were extracted with Triton. Scale bars: 10µm. **B** and **C** are quantification of the results shown in Fig. 5C and Fig. 5D, respectively. Bar graphs indicate the percentage of cells showing cytoplasmic Gli3 protein aggregates. In these experiments, we counted 200 Gli3-transfected cells from each sample.

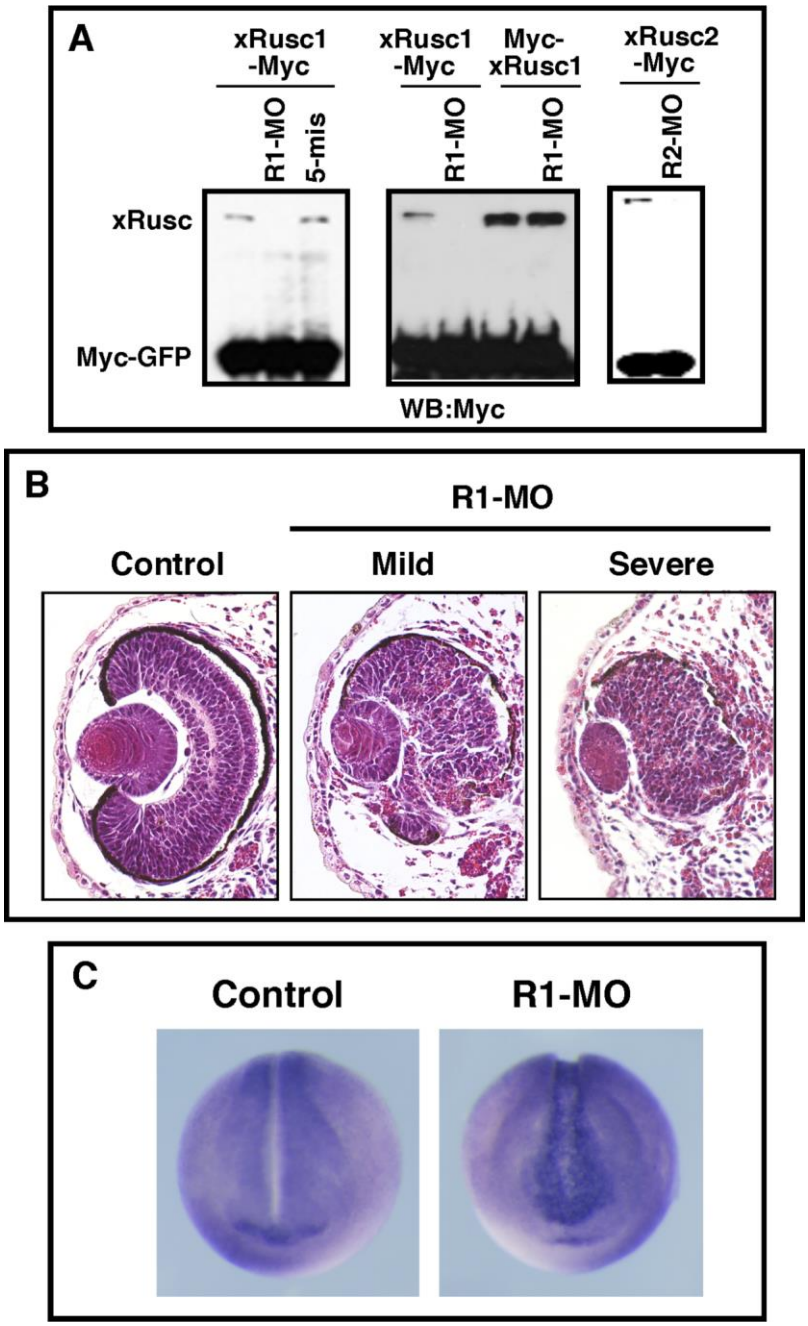

Supplemental Figure 5.

Effects of xRusc morpholinos. A. Western blot showing that injection of Rusc1 morpholino (R1-MO, 20 ng) and Rusc2 morpholinos (R2-MO, 20 ng) into *Xenopus* embryos blocked translation of C-terminal myc-tagged xRusc1 (left panel) and xRusc2 (right panel), respectively. R1-MO blocked translation of a C-terminal myc-tagged xRusc1, but not a N-terminal myc-tagged xRusc1 (middle panel). In these experiments, morpholinos were injected at the 1-cell stage. At the 2-cell stage, a mixture of Rusc (1 ng) and myc-GFP RNA (50 pg)

were injected into embryos. **B**. Histological analysis of eyes from a control embryo (left) and R1-MO injected embryos with mildly (middle) and severely (right) affected eyes. **C**. In situ hybridization showing the expression of *gli1* in a control embryo (left) and an embryo bi-laterally injected with 40 ng of R1-MO (right). Embryos were analyzed at stage 18.

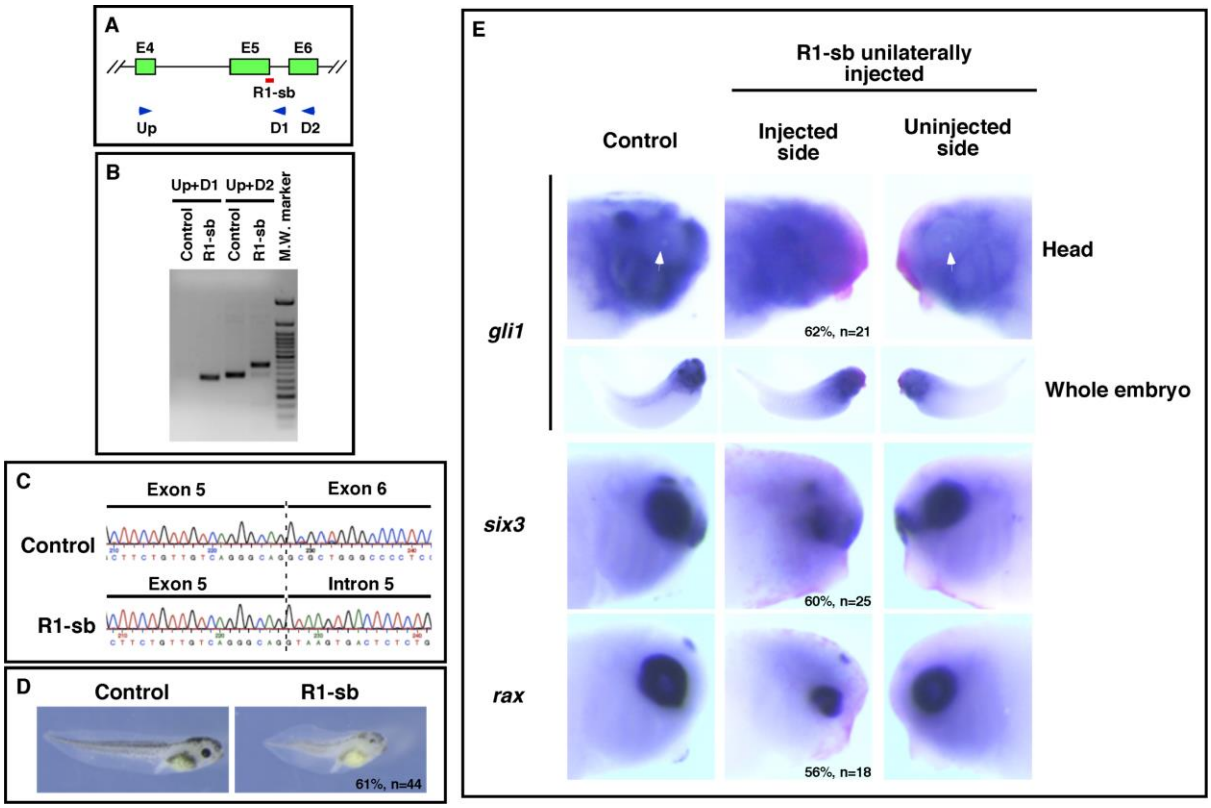

Supplemental Figure 6.

Knocking down xRusc1 by injection of R1-sb enhances Hh signaling and impairs eye development. A. Schematic diagram showing the design of R1-sb, which blocks *rusc1* splicing. Arrowheads indicate primers used in RT-PCR to validate the effect of R1-sb on splicing of *rusc1*. **B.** RT-PCR result showing the effect of R1-sb on *rusc1* splicing. Fertilized eggs were injected with R1-sb (80 ng) and harvested at stage 33 for RT-PCR. **C.** Sequences of the PCR products (primers Up + D1) amplified from control and R1-sb injected embryos, showing insertion of intron 5 into *rusc1* mRNA in R1-sb injected embryos. **D.** Whole embryo morphology of a control tadpole and a tadpole that was injected with 20 ng of R1-sb bilaterally at the 4-cell stage. Both dorsal blastomeres were injected. **E**. In situ hybridization showing the expression of *gli1*, *six3*, and *rax* in control and R1-sb injected embryos. A mixture of R1-sb (20ng) and RNA encoding n-ß-gal (500 pg) was injected into one of the dorsal blastomeres at the 4-cell stage. Embryos were harvested at stage 33. Both un-injected and injected sides of injected embryos are shown. In stage 33 control embryos, *gli1* is not expressed in the eye, forming a prominent "*gli1*-free" domain in the head (pointed by arrows). In R1-sb injected embryos, the *gli1*-free domain disappears. Cells in the head region express *gli1* nearly uniformly.

Supplemental Figures

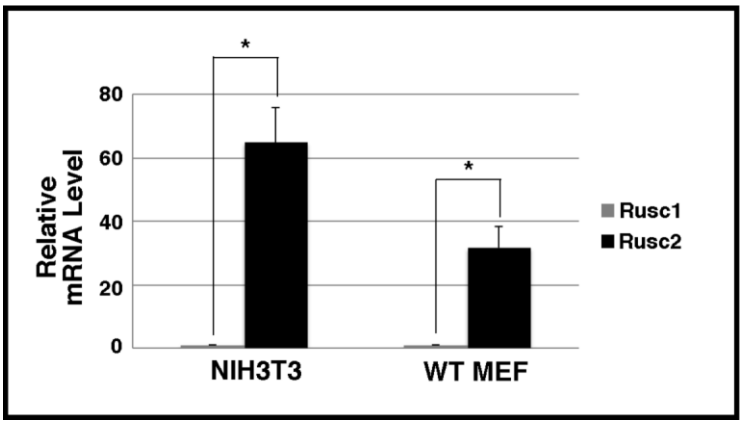

Supplemental Figure 1.

Expression of *rusc1* and *rusc2* in MEFs and NIH3T3 cells. Real-time RT-PCR showing that *rusc2*, but not *rusc1*, is abundantly expressed in NIH3T3 and MEFs. In the real-time PCR experiment, pCS2-Rusc1 and pCS2-Rusc2 plasmids (0.4 pg) were used as the control for normalization. Data are shown as mean±SD. *$p<0.05$.

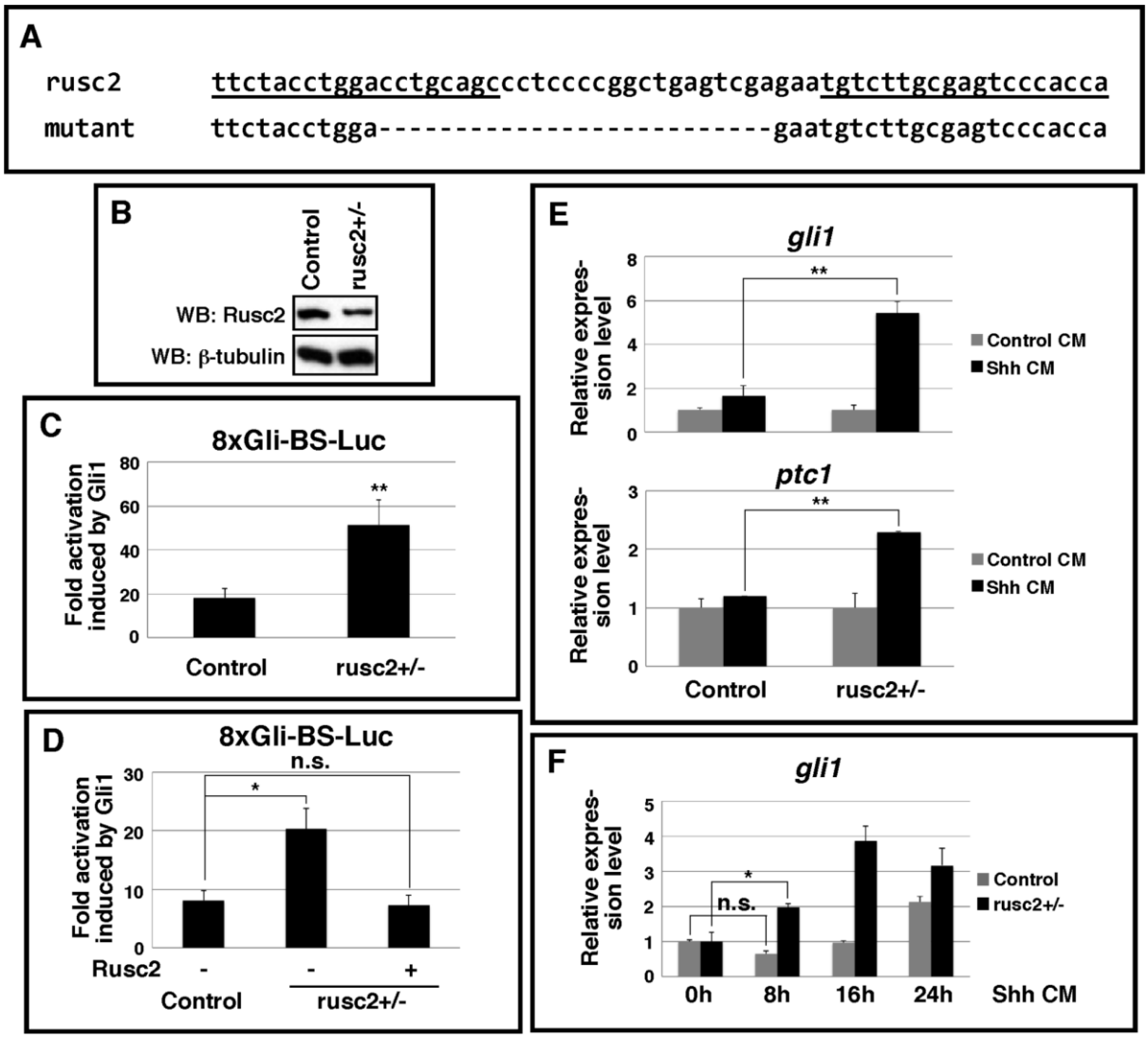

Supplemental Figure 2.

Enhanced Hh response in rusc2 heterozygous mutant MEFs. A. Schematic diagram showing the sequences of the wild type and mutant rusc2 alleles. Sequences targeted by the left and right TALEN arms are underlined. To establish rusc2 mutant cell lines, wild type MEFs were transfected with TALEN and selected by puromycin. Several cell lines were established from TALEN-transfected single cells. The targeted loci of these cells were sequenced. A cell line carrying a mutated rusc2 allele was identified. When testing the Hh response of this rusc2 heterozygous mutant MEF cell line, we used an un-mutated MEF cell line established through the same procedure as the control. **B.** Western blot to show that the expression of Rusc2 is reduced in rusc2 heterozygous mutant MEFs. **C.** Dual-luciferase assay showing that transfection of Gli1 (100 ng) into control MEFs activated the 8xGli-BS-Luciferase reporter by 19 folds. In the rusc2 heterozygous mutant MEFs, the

same amount of Gli1 activated the 8xGli-BS-Luciferase reporter by 51 folds. Data is shown as mean±SD. **p<0.01. **D.** Overexpression of FLAG-hRusc2 rescued the response of the rusc2 heterozygous mutant MEFs to Gli1 in an 8xGli-BS-Luciferase reporter assay. Data is shown as mean±SD. *p<0.05, n.s., non-significant. **E**. Real-time RT-PCR results showing that a low dose of Shh-conditioned medium, which was insufficient for activating *gli1* and *ptc1* expression in control MEFs, markedly increased the expression of *gli1* and *ptc1* in rusc2 heterozygous mutant MEFs. Data is shown as mean±SD. **p<0.01. **F**. Real-time RT-PCR results showing the expression of *gli1* in control and rusc2 heterozygous mutant MEFs at various time points after Shh conditioned medium treatment. Compared to control MEFs, rusc2 heterozygous mutant MEFs showed accelerated *gli1* activation kinetics in response to Shh conditioned medium treatment. Data is shown as mean±SD. *p<0.05, n.s., non-significant.

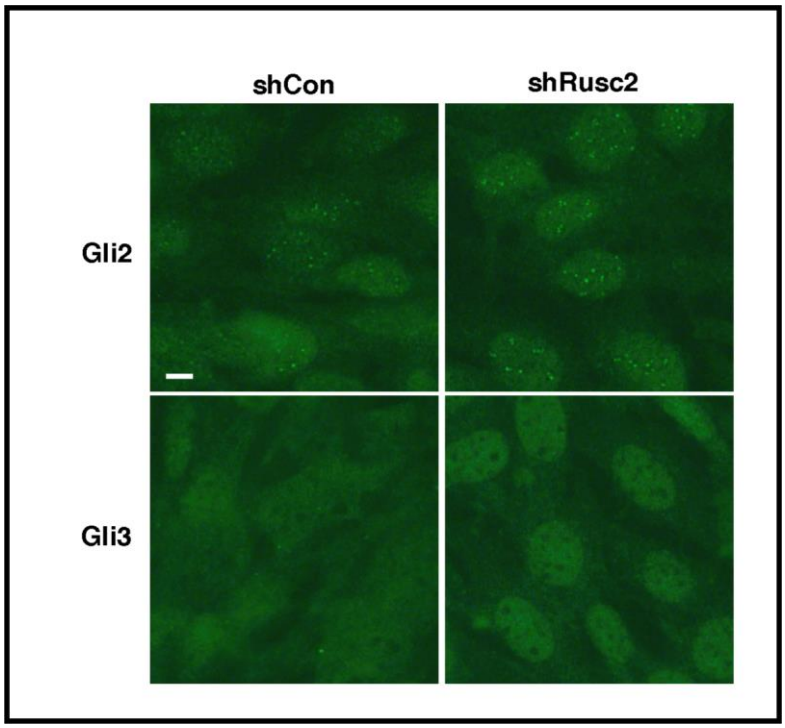

Supplemental Figure 3.

Knockdown of rusc2 does not significantly alter the subcellular localization of endogenous Gli2 and Gli3. Immunofluorescence showing subcellular localization of endogenous Gli2 (upper panels) and Gli3 (lower panels) in control shRNA (left) and Rusc2 shRNA infected cells. Scale bars: 10μm.

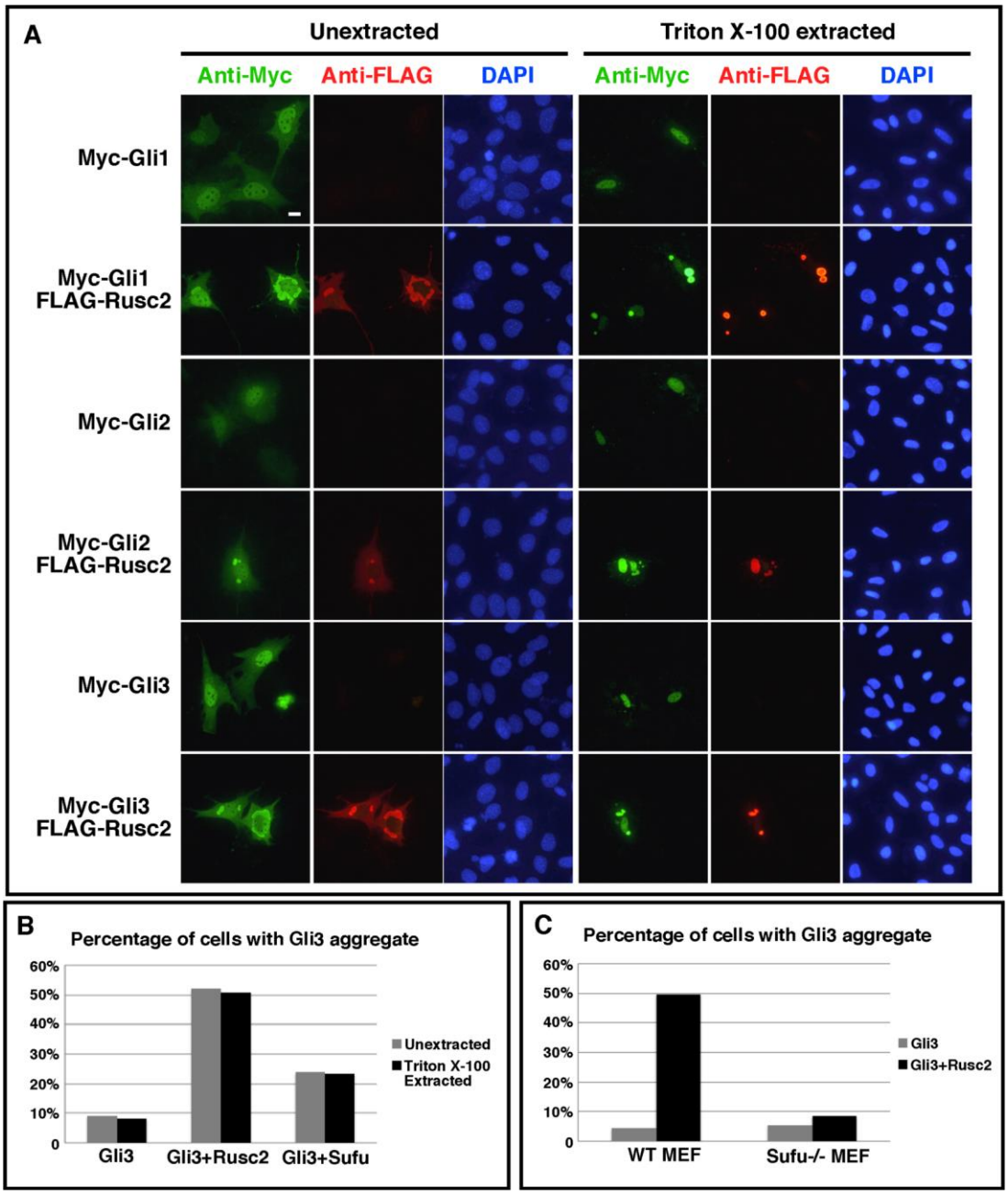

Supplemental Figure 4.

Overexpression of rusc2 induces cytoplasmic Gli1, Gli2, and Gli3 protein aggregates, which are resistant to Triton X-100 extraction. A. Immunofluorescence showing that overexpression of Rusc2 altered the subcellular distribution of myc-Gli1, myc-Gli2, and myc-Gli3 in NIH3T3 cells. When expressed alone, Gli proteins were enriched in the nucleus. Overexpression of hRusc2 decreased the amount of Gli proteins in the nucleus and induced cytoplasmic Gli protein aggregates. In the Triton extraction experiment, cells were pre-extracted with 0.5% Triton X-100 in a cytoskeleton stabilizing buffer for 3 minutes at 4°C

prior to fixation. This treatment condition was sufficient for removing all cytosolic GFP in myc-GFP transfected cells (not shown). However, Gli protein aggregates remained in the cytoplasm after cells were extracted with Triton. Scale bars: 10µm. **B** and **C** are quantification of the results shown in Fig. 5C and Fig. 5D, respectively. Bar graphs indicate the percentage of cells showing cytoplasmic Gli3 protein aggregates. In these experiments, we counted 200 Gli3-transfected cells from each sample.

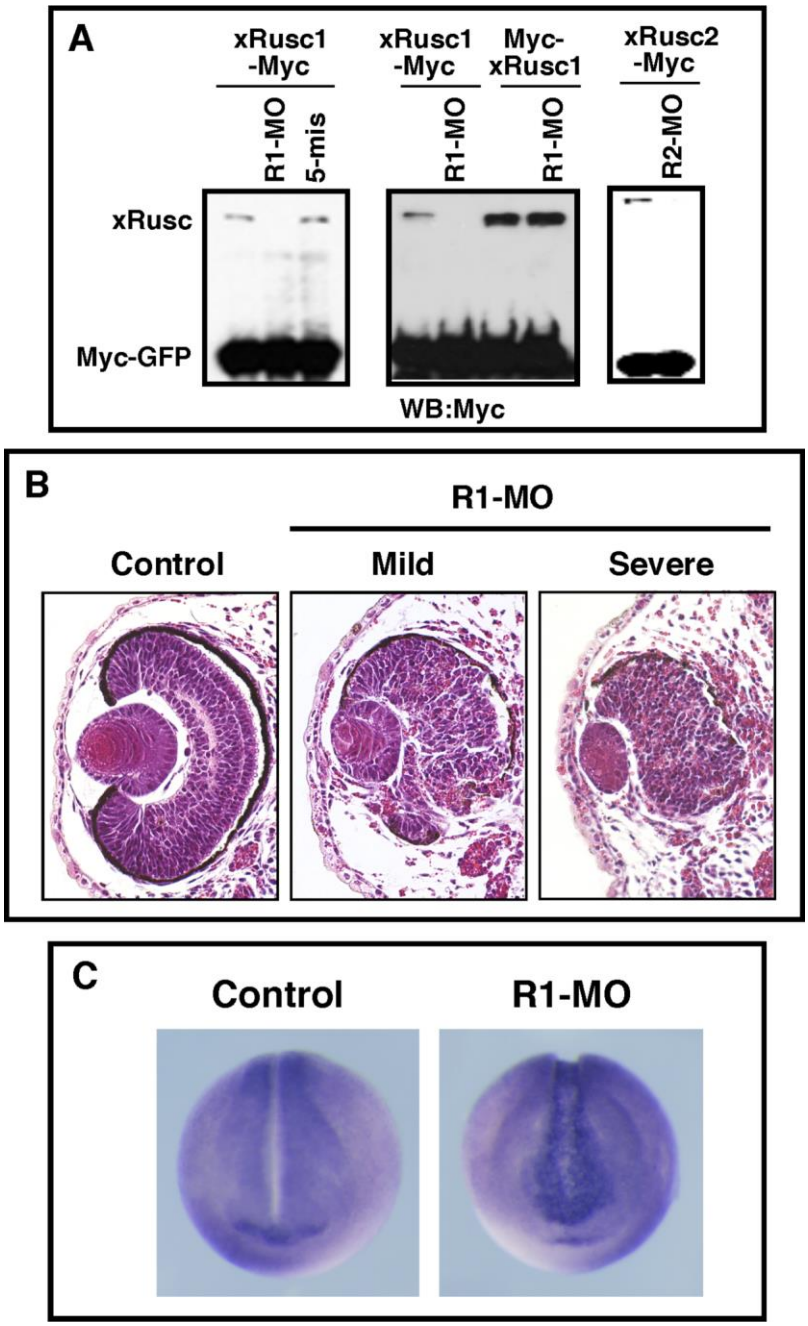

Supplemental Figure 5.

Effects of xRusc morpholinos. A. Western blot showing that injection of Rusc1 morpholino (R1-MO, 20 ng) and Rusc2 morpholinos (R2-MO, 20 ng) into *Xenopus* embryos blocked translation of C-terminal myc-tagged xRusc1 (left panel) and xRusc2 (right panel), respectively. R1-MO blocked translation of a C-terminal myc-tagged xRusc1, but not a N-terminal myc-tagged xRusc1 (middle panel). In these experiments, morpholinos were injected at the 1-cell stage. At the 2-cell stage, a mixture of Rusc (1 ng) and myc-GFP RNA (50 pg)

were injected into embryos. **B**. Histological analysis of eyes from a control embryo (left) and R1-MO injected embryos with mildly (middle) and severely (right) affected eyes. **C**. In situ hybridization showing the expression of *gli1* in a control embryo (left) and an embryo bi-laterally injected with 40 ng of R1-MO (right). Embryos were analyzed at stage 18.

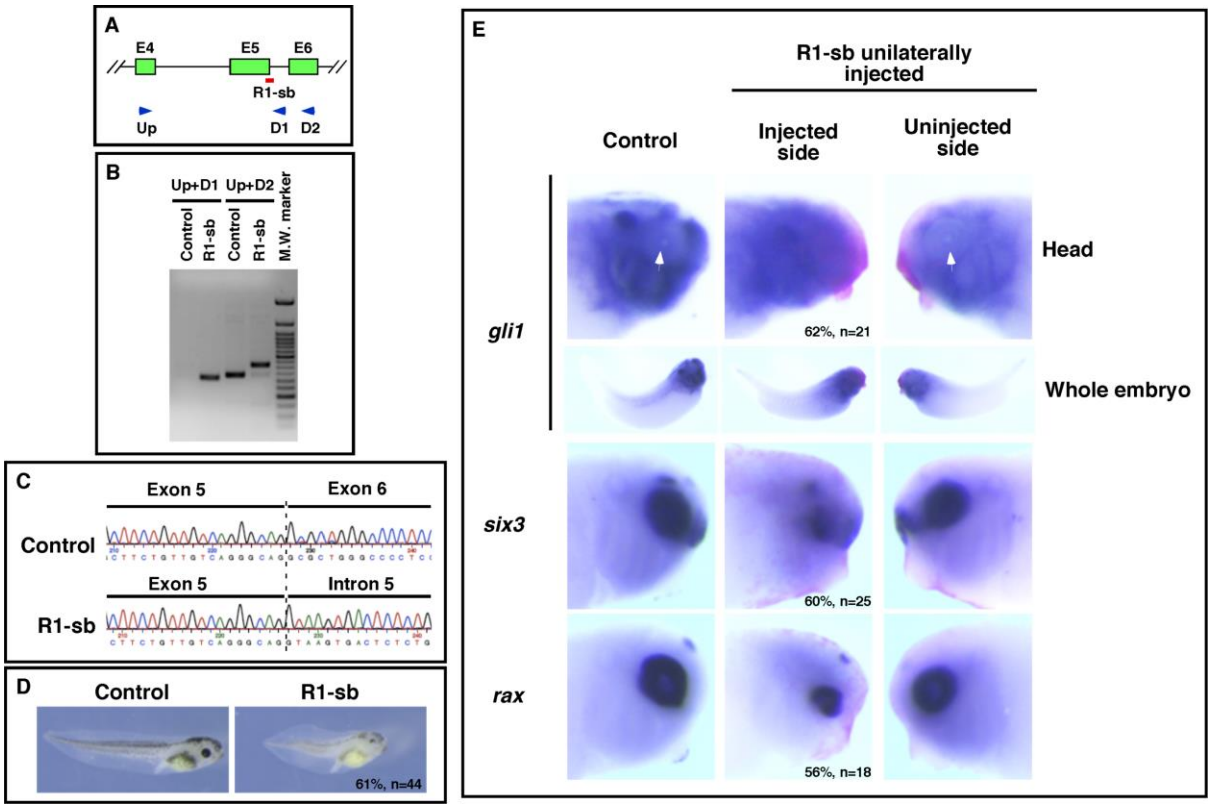

Supplemental Figure 6.

Knocking down xRusc1 by injection of R1-sb enhances Hh signaling and impairs eye development. A. Schematic diagram showing the design of R1-sb, which blocks *rusc1* splicing. Arrowheads indicate primers used in RT-PCR to validate the effect of R1-sb on splicing of *rusc1*. **B.** RT-PCR result showing the effect of R1-sb on *rusc1* splicing. Fertilized eggs were injected with R1-sb (80 ng) and harvested at stage 33 for RT-PCR. **C.** Sequences of the PCR products (primers Up + D1) amplified from control and R1-sb injected embryos, showing insertion of intron 5 into *rusc1* mRNA in R1-sb injected embryos. **D.** Whole embryo morphology of a control tadpole and a tadpole that was injected with 20 ng of R1-sb bilaterally at the 4-cell stage. Both dorsal blastomeres were injected. **E**. In situ hybridization showing the expression of *gli1*, *six3*, and *rax* in control and R1-sb injected embryos. A mixture of R1-sb (20ng) and RNA encoding n-ß-gal (500 pg) was injected into one of the dorsal blastomeres at the 4-cell stage. Embryos were harvested at stage 33. Both un-injected and injected sides of injected embryos are shown. In stage 33 control embryos, *gli1* is not expressed in the eye, forming a prominent "*gli1*-free" domain in the head (pointed by arrows). In R1-sb injected embryos, the *gli1*-free domain disappears. Cells in the head region express *gli1* nearly uniformly.